Bernhard Sölle,BSc

Perylene functionalized epoxy resins

MASTER'S THESIS

to achieve the university degree of

Diplom-Ingenieur

Master's degree programme:

Technical chemistry

submitted to

Graz University of Technology

Supervisor

Univ.-Prof. Dipl.-Ing. Dr.techn. Gregor Trimmel

Institut für chemische Technologie von Materialien

Graz, March 2021

AFFIDAVIT

I declare that I have authored this thesis independently, that I have not used other than the declared sources/resources, and that I have explicitly indicated all material which has been quoted either literally or by content from the sources used. The text document uploaded to TUGRAZonline is identical to the present master's thesis.

Date, Signature

Abstract

Heat dissipation in electronic devices is becoming increasingly important, as the performance of these devices increases day by day while the size decreases. Polymers generally have low thermal conductivities. To increase the thermal conductivity, usually aromatic polymers are used and especially ones that can undergo π-π stacking are very promising, which makes perylene derivatives potential candidates to achieve that goal.

This work deals with the synthesis and characterization of different perylene derivatives, as well as their use to cure epoxy monomers.
Two approaches were carried out.

First the ability of perylene tetracarboxylic acid dianhydride (**PTCDA**) to act as curing agent was investigated.
Different PTCDA derivatives were synthesized, characterized, and used to cure epoxy monomers. All reaction attempts have shown that it was not possible to obtain a crosslinked insoluble resin. It is believed that only hydrolysis of the anhydride took place, and that the epoxide underwent homopolymerization.

In a second approach, two different amine functionalized perylenediimide (**PDI**) derivatives were synthesized and characterized. Both were successfully used to cure epoxy monomers.
Whereas the first only had one amine functionality the polymerization reaction led to linear chains and the polymer stayed soluble.
The second PDI-derivative, featuring two primary amine functionalities, built an infusible three-dimensional network.

The electrical and photoconductivity of these polymers were tested in a photovoltaic device structure.

Kurzfassung

Die Wärmeableitung in elektronischen Geräten wird immer wichtiger, da die Leistung dieser Geräte von Tag zu Tag steigt, während sie in ihrer Größe schrumpfen. Polymere haben im Allgemeinen niedrige Wärmeleitfähigkeiten. Um die Wärmeleitfähigkeit zu erhöhen, werden in der Regel Polymere mit aromatischen Gruppen verwendet und insbesondere solche, die eine π-π-Stapelung eingehen können, sind sehr vielversprechend, was Perylenderivate zu potenziellen Kandidaten macht, um dieses Ziel zu erreichen.

Diese Arbeit befasst sich mit der Synthese und Charakterisierung verschiedener Perylenderivate, sowie deren Verwendung zur Aushärtung von Epoxidmonomeren.
Es wurden zwei Ansätze durchgeführt.

Zunächst wurde die Fähigkeit von Perylentetracarbonsäuredianhydrid (**PTCDA**) untersucht, um als Härter für Epoxyharze zu fungieren.
Verschiedene PTCDA-Derivate wurden synthetisiert, charakterisiert und zur Aushärtung von Epoxidmonomeren verwendet. Alle Reaktionsversuche haben gezeigt, dass es nicht möglich war, ein vernetztes unlösliches Harz zu erhalten. Es wird angenommen, dass nur eine Hydrolyse des Anhydrids stattfand und das Epoxid nur eine Homopolymerisation durchlief.

In einem zweiten Ansatz wurden zwei verschiedene aminfunktionalisierte Perylendiimid (**PDI**) Derivate synthetisiert und charakterisiert. Beide wurden erfolgreich zur Aushärtung von Epoxidmonomeren eingesetzt.
Während das erste nur eine Aminfunktionalität aufwießt, führte die Polymerisationsreaktion zu linearen Ketten und das Polymer blieb löslich.
Das zweite PDI-Derivat, das zwei primäre Aminfunktionalitäten aufwieß, bildete ein unschmelzbares dreidimensionales Netzwerk.

Die Polymere wurden hinsichtlich ihrer elektrischen und photelektrischen Eigenschaften in einem Solarzellenaufbau getestet.

Acknowledgement

At this point I want to thank all people that helped making this thesis possible.
First of all, I want to thank Professor Gregor Trimmel, my supervisor, for giving me the opportunity to do my thesis at the institute and his support.
Also, I want to address my special thanks to Dr. Matiss Reinfelds, who helped me throughout all parts of the thesis with his knowledge and his always positive attitude.
Furthermore, thanks to my working group for their help and friendly working atmosphere.
Besides university, I want to thank my friends and family for their support.

Table of Contents

1. Introduction

The rapid development of miniaturizing electronic devices and their increase in performance makes a better heat dissipation way more important.[1]

One of the most common materials for electronic packaging are epoxy resins. They show good mechanical properties, they are cheap and lightweight and can protect the electronic device from moisture and mechanical damage. The major disadvantage is their generally low thermal conductivity.[2–4]

The weak molecular interactions and structural disorders in polymers seems to be the reason for the generally bad thermal conducting performance (~0.2 W/mK).[5]

Several approaches have been made to increase the thermal conductivity of polymers by improving the alignment of the molecular chains. For example by drawing of polyethylene nanofibers the thermal conductivity could be increased from 0.5 W/mK to 100 W/mK.[6,7] With this method the intramolecular thermal conductivity along the polymer backbone could be increased, however the intermolecular conductivity is still low.[8]

Conjugated polymers are considered to show good thermal conducting behavior, due to the conjugated backbone and the intermolecular π-π stacking. The π-π stacking is much stronger then Van der Waals interactions in “normal“ polymers and therefore the phonon scattering is suppressed. [8,9]

Perylene derivatives show good thermal resistance and are able to self-assemble due to π-π stacking.[10] Therefore they are potential candidates for improving the thermal stability and thermal conductivity of a polymer.

Thus, the central goal of this work was, to prepare perylene functionalized epoxy resins. Perylene would increase the thermal conductivity through its aromatic character. In addition, the strong absorption and fluorescence make them interesting materials in optics.

In a first approach different perylene tetracarboxylic dianhydrides were investigated as possible curing agents for epoxy monomers since these compounds are commercially available.

Furthermore, as alternative approach, the focus of investigations was set on the synthesis of amine functionalized perylene derivatives and their use to cure epoxides. The resulting resins then were investigated in regard to their photovoltaic performance.

2. Theoretical part

2.1 Epoxy resins

2.1.1 History

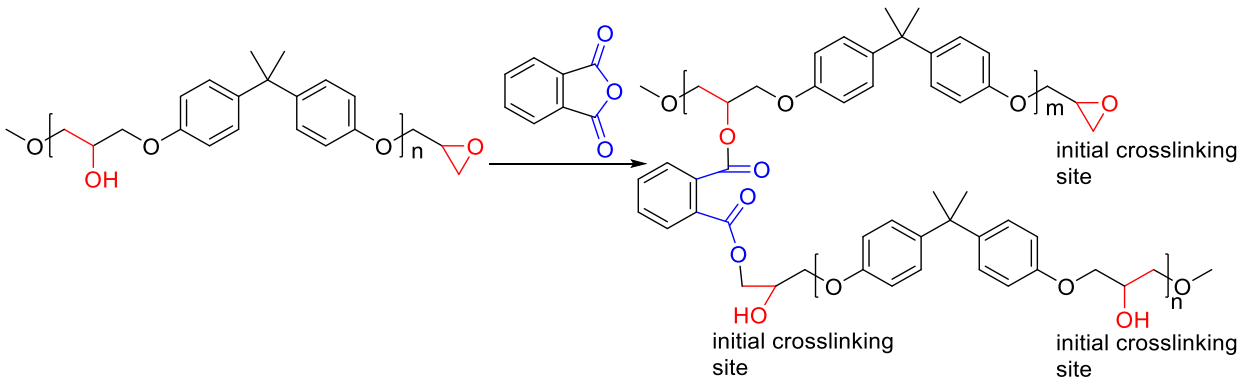

Figure 1: First resin synthesis. Showing the uncured and cured resin.

Epoxy resins are synthetic resins that either still contain epoxide groups as reactive center or are already cured compounds where the epoxide was opened in the curing reaction. Industrially these polymers are of very great importance because of their properties. They are very robust, have a low volume change during curing, are resistant against most solvents and acids and they show good adhesion on most surfaces. Therefore, they are used in a wide range of different applications such as for paints and coatings, electronics, composites, wind turbines, construction, and adhesives. One of them is becoming increasingly important, namely the electrical and electronics sector.[11,12,13]

The synthesis of the first epoxy resin can be traced back to 1891. In the 1940s they became commercially available because of the work of Pierre Castan in Switzerland and Sylvan Greenlee in the United States, which worked in two different companies and searched independently on epoxy formulations.[13]

One of the first resins ever synthesized was a thermoset composition of epichlorohydrin and bisphenol-A cured with phthalic anhydride. After the Second World War, epoxy resins gained great interest. The first applications were surface coatings and they are still widely used in this field today.[14]

The research in bisphenol-A based epoxy resins was intensified by two U.S. companies in the late 1940s. Over the years, companies began to modify the properties of epoxy resins in order to obtain substances that could be used in an even wider field.[14]

2.1.2 Curing of Epoxy resins

Epoxy resin educts need to be cured, in other words crosslinked, to obtain their chemical and physical properties. The three-dimensional and infusible network that is built up is the reason for the performance of the resin. One needs to differ between two main types of curing agents, catalytic or co-reactive ones. Catalytic curing agents open up the oxiran ring and promote epoxy homopolymerization. Whereas co-reactive ones are taking part as co-monomers. The last mentioned are considered to be the more important ones. [15]

Both electrophiles and nucleophiles are able to cure epoxy resins, the most important ones are amines and anhydrides. Depending on which system chosen, one can alter the properties of the resin significantly. It is also important to choose the right curing agent for the right processing method and curing conditions.[15]

Amine curing is usually done at lower temperatures and is therefore referred to as cold curing system. Anhydride curing therefore is done at elevated temperatures and usually a catalyst is required. Therefore, it can be said that the anhydride cured systems are much more complex. [16]

Curing with amines

The most widely used curing agents are primary and secondary amines. The reaction rates of those are usually very fast. However, the reaction rate is influenced by steric and electronic properties of the nucleophile. For example, electron donating groups support the nucleophilic character of the amine and increases the reaction rate. Primary amines react faster than secondary ones. [15]

In theory, each primary amine can react with two epoxy groups. First the primary amine is reacted, and a secondary amine gets formed, which then can react further with another epoxide group resulting in a polymeric chain. To obtain crosslinked and infusible polymers one need to use at least a diamine and a diepoxide.[13,17]

The most important reactions taking place can be seen Figure 2.

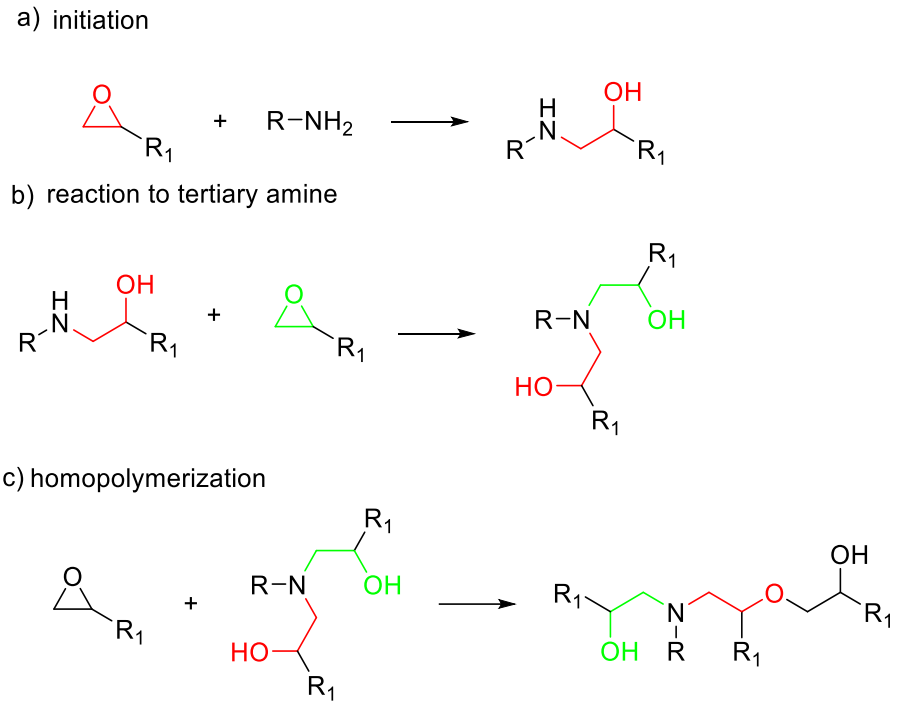

Figure 2:Main reaction schemes of the polymerization of an epoxide with an amine
a) initial step b) crosslinking reaction with diamine c) competing reaction (homopolymerization of epoxide)

Figure 2a shows the initial step. The epoxide reacts with a primary amine and a secondary amine and a secondary alcohol is produced. After a stoichiometric amount of amine reacted, the generated secondary amines will react with an additional epoxy-group to form a tertiary amine and a second secondary alcohol.
Alternatively, the secondary alcohols can react with another epoxide group and form an ether. This competitive reaction is favored at higher temperatures. The reaction scheme can be seen in Figure 2c.

The first amine-based curing agents were aliphatic polyamines, because curing at room temperature with bisphenol-A type epoxies can be easily done. But disadvantages are, that most of them are volatile and hygroscopic, smell bad and they can cause dermatitis. Therefore, modifications of the amines have been carried out. Nowadays unmodified polyamines are mostly used to produce epoxy adducts. The obtained products are easier to handle. Figure 3 shows an example.[14]

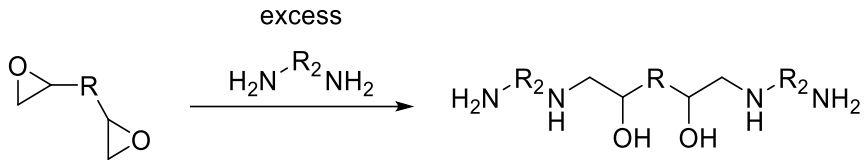

Figure 3: example of an epoxy adduct

Curing with anhydrides

Cyclic anhydrides are the second major class of curing agents for epoxy resin. [17]

The properties of the anhydride cured epoxy resins are usually better than those of the amine cured ones. The reaction can be carried out in a matter that no hydroxyl groups are present in the cured resin. Due to this fact, they are less prone to absorb polar substances (e.g., water), which gives them an advantage compared to amine cured resins. Furthermore they usually have higher glass transition temperatures and lower toxicities than amine cured ones. [18]

A disadvantage of most anhydride-epoxy curing reactions is their lower reactivity and therefore relatively high reaction temperatures are needed.

The uncatalyzed epoxy/anhydride reaction was the first one investigated according to the mechanism by Fisch et. al. They discovered that the uncatalyzed reaction requires the presence of hydroxyl groups. [19]

In Figure 4 the reaction schemes of the uncatalyzed system can be seen.

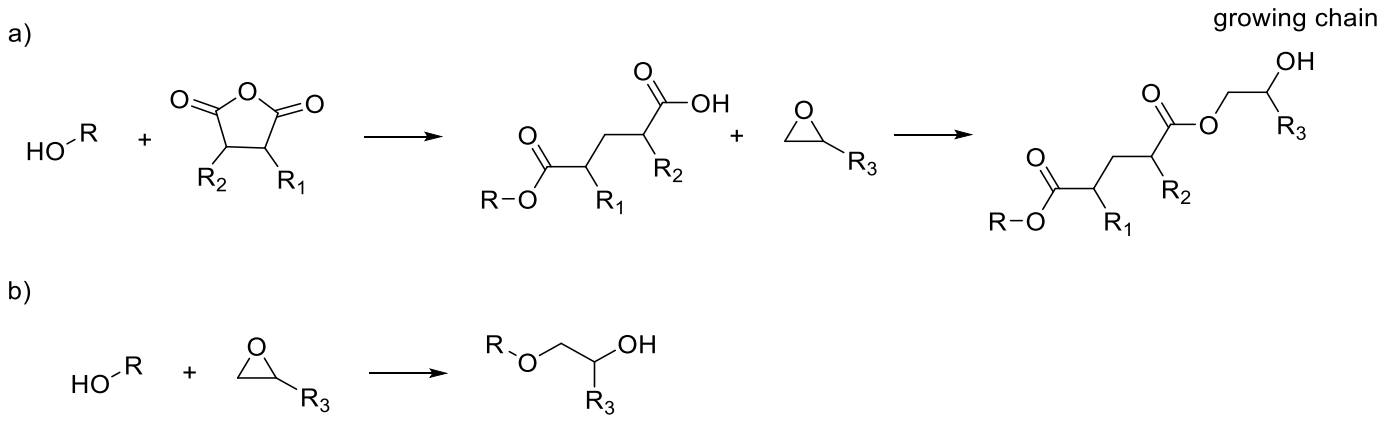

Figure 4: Reaction scheme of uncatalyzed epoxy anhydride systems
a) Reaction of secondary alcohol of the resin with anhydride to produce a monoester, the generated carboxyl group reacts with the epoxide to form a diester
b) Homopolymerization of the epoxides

It was recognized that epoxy groups decreased at higher rate than the diester groups did form. This led to the conclusion, that some side reactions have to take place. Fisch

and Hofmann stated that at the uncatalyzed system esterification and etherification take place at almost same extent and that the etherification (homopolymerization) is catalyzed by the presence of the anhydride or the carboxylic acid.[20]

Since the uncatalyzed reaction showed the formation of random polymers, soon it has been discovered, that Lewis bases, such as tertiary amines, not only are able to catalyze the polymerization reaction but also suppresses the ether formation.[21]
It is still not exactly clear how the initiation process of the base catalyzed reaction works. Different authors proposed different mechanisms, which can be narrowed down to three different approaches.[22]

- Ionic mechanism according to Fischer
- Initiation with preexisting proton donor
- Mechanism according to Tanaka, where the proton Donor arises in the reaction

Fischer was one of the first researchers that described the selectivity of the reaction when a tertiary amine is present. He showed, that when equimolar quantities of phthalic anhydride and allyl glycidylether are brought to reaction at 100° C, the residual acidity at the end of the reaction is less than 1 %. This means that 99 % of the epoxide molecules react with an anhydride molecule before reacting with its own. [21]

According to Fischer, the base catalyzed reaction is initiated by the ring opening of the anhydride by a tertiary amine. The amine nucleophilic attacks the anhydride forming a quaternary ammonium salt and a carboxylate anion. The participating amine is deactivated.

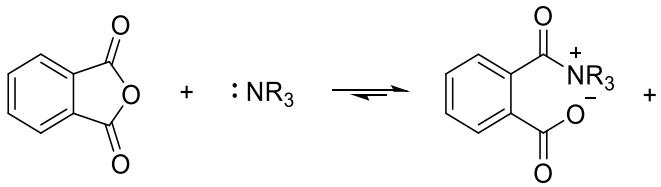

Figure 5: Initiation step according to Fischer

The formed species now reacts with the epoxide to form an ester and creates an alkoxide anion. The anion reacts at a very fast rate with another anhydride creating again a carboxylate anion and the polymeric chain is growing.

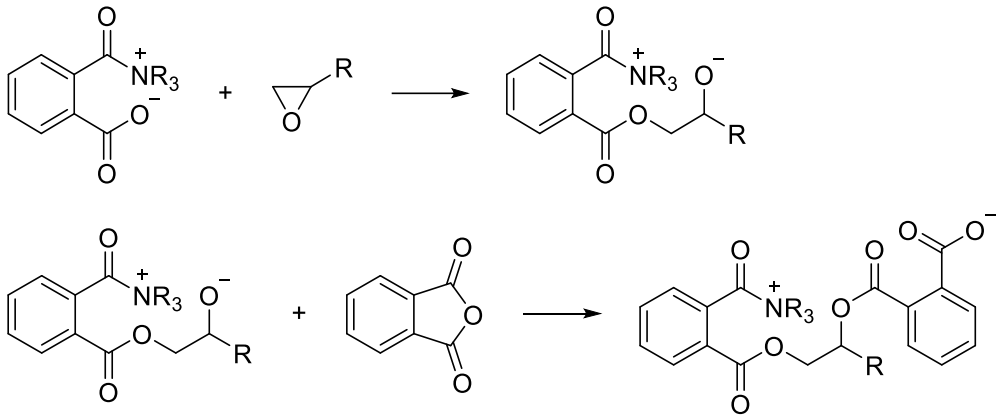

Figure 6: Propagation step

As long as the initiating molecule stays attached the number of growing chains is the same as the one of the initiating molecules. Therefore, the reaction of an anhydride with an epoxide can be seen as living anionic polymerization.[23]
It has been reported that the molecular weights are lower than those expected for an ideal living polymerization. Steinmann B. showed that this fact is due to chain transfer reactions as shown in Figure 7.[24]

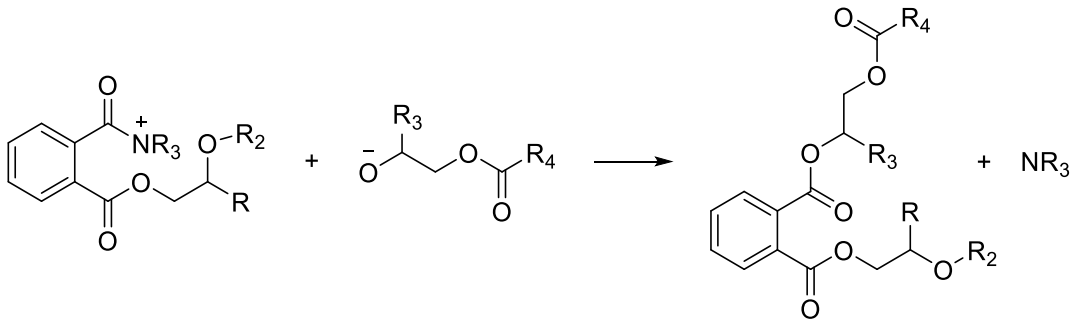

Figure 7: Chain transfer and regeneration of the tertiary amine

The anion of another chain can attack the carbonyl carbon with the attached tertiary amine. Therefore, one polymer chain gets transferred to another and the tertiary amine gets regenerated and can initiate the growing of a new polymer chain.

Tanaka and Kakiuchi studied the kinetics of the tertiary amine catalyzed epoxy anhydride reaction and proposed a mechanism where proton donors, such as -OH groups, act as co catalyst. [25,26]

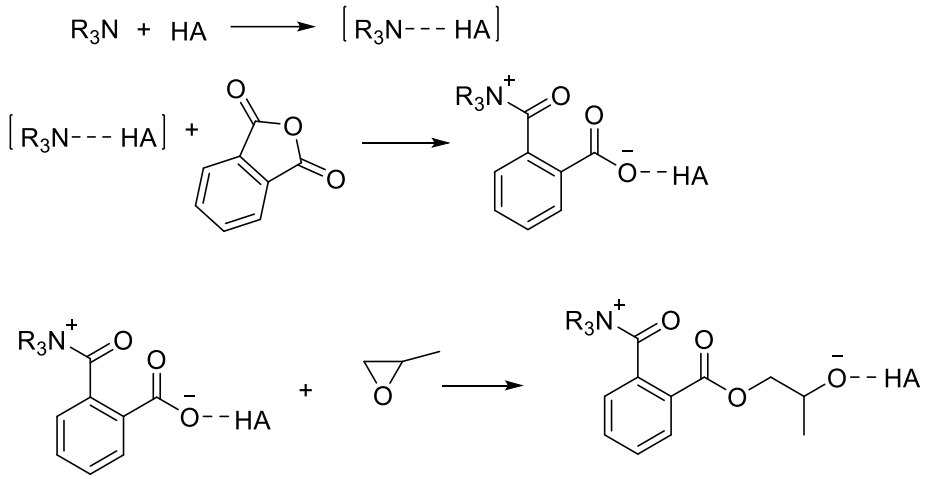

Figure 8: Mechanism of the epoxy/anhydride reaction according to Tanaka and Kakiuchi where HA is a proton donor

There are many similarities between all these proposed mechanisms, but to the best of the knowledge of the author of this work, there is no generally accepted one that takes into account all the peculiarities found by the researchers.

All authors agree that polymerization occurs via an anionic mechanism and that the tertiary amine suppresses epoxide homopolymerization.

2.2 Properties and applications of perylene derivatives

Perylene derivatives are an important class of materials and have been originally used as dyes and pigments. The synthesis of those derivatives usually starts with the insoluble perylene tetracarboxylic acid dianhydride (**PTCDA**).[27]

PTCDA has, due to its insolubility, only a limited number of applications. Therefore, when dealing with perylenes, mostly perylene tetracarboxylic acid diimides (**PDI**) are used. They show high thermal stability, easy tuneability, high photochemical stability and good electron accepting character, which opens a wide spectrum of different applications. For example, they are used in organic field effect transistors, fluorescent solar collectors, dye lasers , organic photovoltaics and as organic battery materials.[28]

Usually perylenes are tuned by modification of the bay position of the aromatic core and the N,N´ positions (Figure 9).

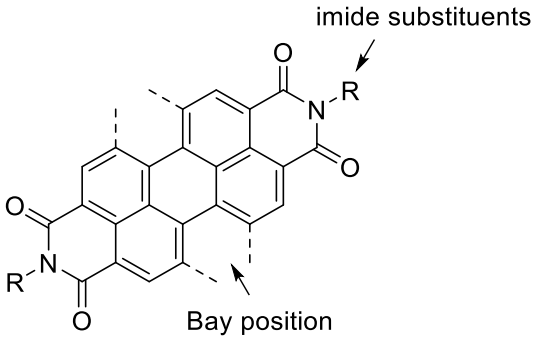

Figure 9: Structure of perylene diimide

Whereas modification of the bay region has a stronger effect on the electronical and optical properties, the imide substituents can be used to affect the aggregation and solubility of the dyes.[28]

Furthermore PDI-derivatives show two reversible one electron redox reactions. In the first step one carbonyl oxygen is reduced to form a radical anion (**PDI**$^{\cdot-}$). In a second reduction process the dianion (**PDI**$^{2-}$) is formed.[29,30]

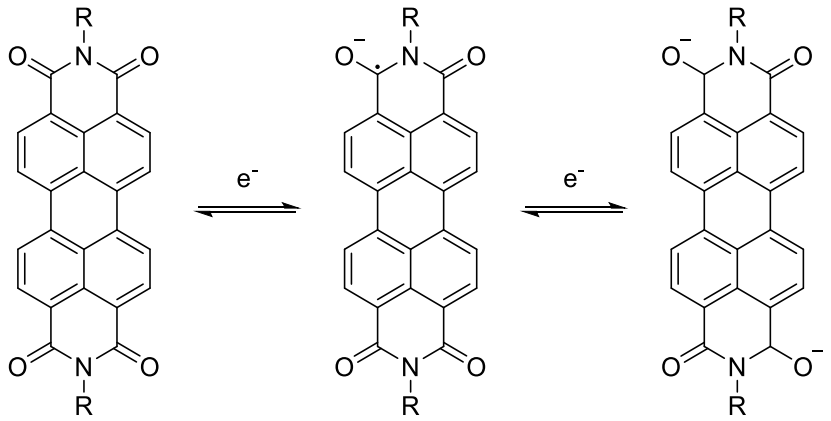

Figure 10: Redox behavior of perylene diimides.

PDI´s gained a lot of interest as accepting materials in OPV´s, due to their advantages compared to fullerene acceptors. They find use not only as small molecule accepting materials, but were also incorporated into polymers, to build all polymer solar cells. For example, Xiong et. al. reported all polymer solar cells, were the perylene polymerizes over the bay position, with power conversion efficiencies of 4.47% (**PDI-I**) [31]. Ying et. al. have reported fused PDI polymers with power conversion efficiencies of 6.58%(**PDI-II**).[32]

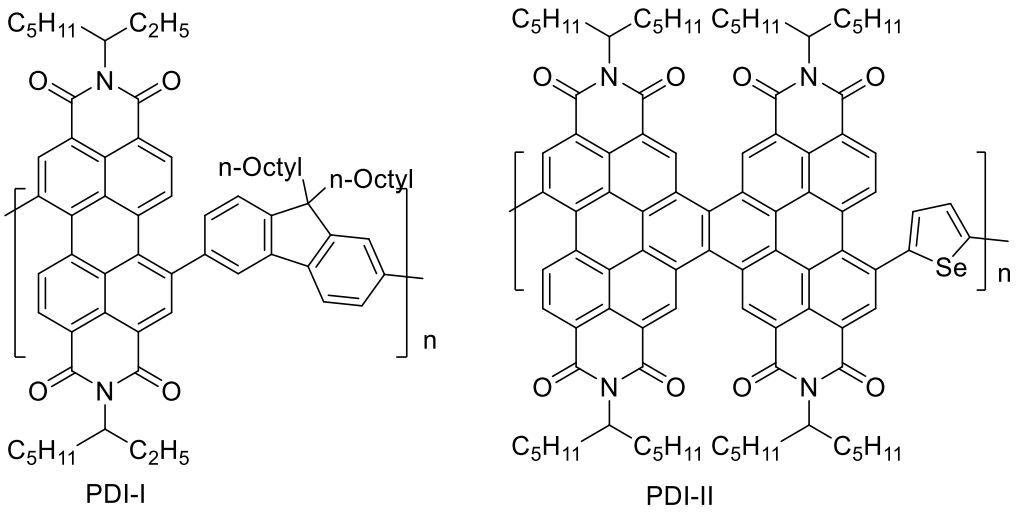

Figure 11: Structure of PDI´s for all polymer solar cells

A few authors also described the use of perylene derivatives in epoxy resins to tune their properties.

For example, Kolcu et. al. showed the synthesis of soluble poly(epoxy-ether)s bearing perylene units. They showed that the amine cured resins had high glass transition values (T_g) and were stable up to temperatures of 329°C which makes them useful for high performance application (e.g. aerospace and electronic industries). [33]

In 2014 Pan et. al. showed that the mechanical and thermal properties of epoxy resins could be enhanced by adding polyester grafted PDI´s. They have shown that the fracture behavior changes from brittle fractures for the neat epoxy to tough fracture for the modified epoxy. Furthermore they showed that adding 1.5 wt% of the PDI derivative increased the decomposition temperature from 332°C for the neat to 375°C for the modified epoxy.[34]

3. Experimental section

3.1 Chemicals

All chemicals were purchased from commercial sources, except epoxide EP1 which was synthesized by Dr. David Beichl and N-(1-hexylheptyl)amine which was synthesized by Dr. Matiss Reinfelds.
All products were used without further purification unless otherwise stated.

3.2 Methods

Thin layer chromatography

For TLC, silica gel 60 on aluminum sheets from Merck were used. Spots were, if necessary, visualized under UV-light.
For preparative TLC, silica gel 60 on a glass plate from Macherey Nagel was used. The different lines were separated by scratching off the silica gel from the plate and desorbing the product from the silica gel with a proper solvent.

Flash chromatography

Flash chromatographic separation was done with a Biotage selekt system. All columns were self-packed with silica gel 60 from Macherey Nagel unless otherwise stated.

^{1}H and ^{13}C NMR spectroscopy

For NMR spectroscopy a Bruker Avance 300 MHz spectrometer was used. All deuterated solvents (e.g. chloroform-d, DMSO-d_6, benzene-d_6) were purchased from Euriso-top. All spectra were referenced against TMS standard if not stated otherwise.

Thermogravimetric analysis

TGA/DSC was done on a STA Jupiter 449C from Netzsch. The temperature ranged from 20-550°C with a scan rate of 10°C/min. As protective gas helium was used with a flow rate of 50 ml/min. All measurements were performed by Josefine Hobisch.

UV-Vis spectroscopy

All spectra were recorded on a Shimadzu UV-1800. The measurements were done either in solution or as thin film on a glass substrate. A glass cuvette with a thickness of 1 cm was used. The scan rate was 350 nm/min.

IR-spectroscopy

All spectra were recorded on a Bruker Alpha-p FT-IR spectrometer with an ATR device.

J-V curves

The curves were recorded by using a Keithley 2400 source meter. All measurements were carried out inside the glove box. A LabView based software was used to carry out the measurements. As light source a dedolight DLH400D generating an emission spectrum comparable to AM1.5G was used. The illuminated area was defined by a mask and had a size of 0.070225 cm^2.

The measurements were carried out with a light intensity of approximately 100mW/cm^2 and under dark and illuminated conditions as far as this was reasonable.

All scans were measured from -500 to 1500 mV. 100 measuring points were taken with a delay of 100 ms and a step width of -0.02 V.

Film thickness

The film thickness was measured with a Bruker DektakXT stylus profilometer. With a scalpel lines were scratched into the active layer and the thickness of the scratches was measured. The mean of three measurements was taken.

3.3 Synthesis of Nitro-substituted Perlylenedianhydride

3.3.1 1-Nitroperylene-3,4,9,10-tetracarboxylic-dianhydride (PDA-(NO_2))

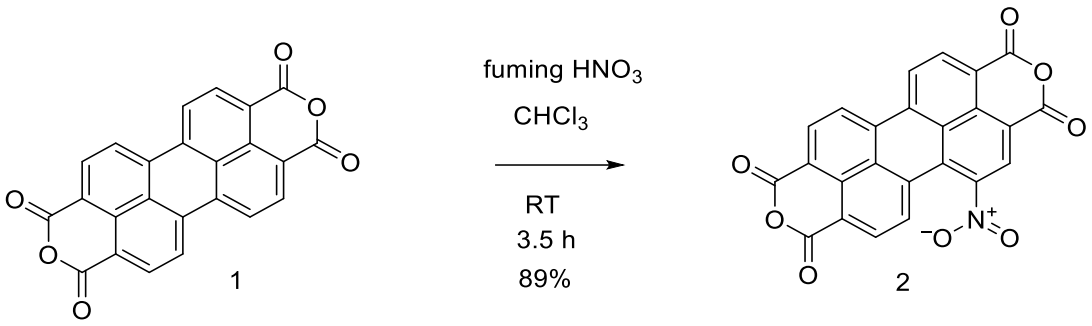

Scheme 1: Preparation of mono-nitrated perylenedianhydride (2)

Perylene-3,4,9,10-tetracarboxylic dianhydride (PDA) (5.03 g; 12.82 mmol) was suspended in chloroform (150 ml) and stirred at room temperature. Fuming HNO_3 >90% (50 ml) was added dropwise over a time period of 20min. The PDA started to dissolve immediately. After 3.5 h the reaction mixture was slowly poured into water (500ml). The precipitate was filtered and washed with water until the filtrate reached a pH-value of approximately 7.

The crude red product was dried under reduced pressure. Since the product has a very low solubility, it could not be purified by silica gel column or recrystallisation. Also, sublimation was tried, but the NMR spectrum showed, that the product was destroyed.

Yield (crude product): 5.64 g (90%)

IR (cm^{-1}): 3064, 1774, 1742, 1599, 1538 (NO_2),1401, 1367, 1340, 1305 (NO_2), 1238, 1151, 1056, 808, 734,706, 565

3.3.2 1,6 and 1,7 Dinitroperylene-3,4,9,10 tetracarboxylic dianhydride (PDA-$(NO_2)_2$) isomeric mixture

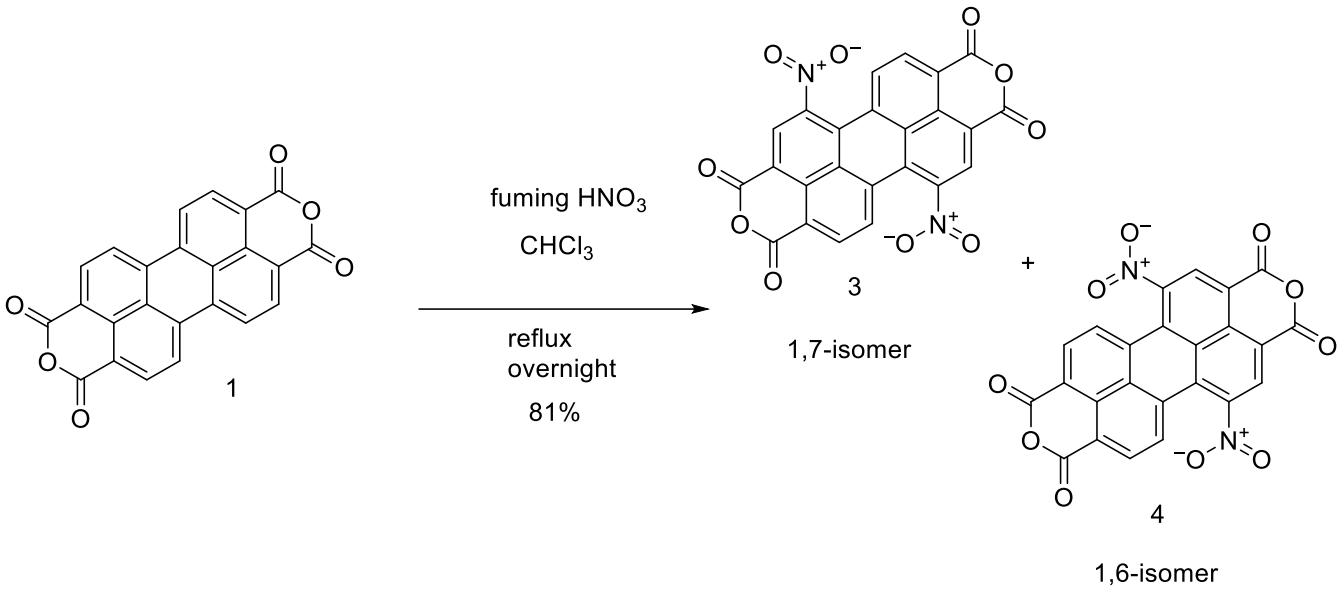

Scheme 2:Preparation of di-nitrated perylenedianhydride (3,4)

Perylene-3,4,9,10-tetracarboxylic dianhydride (PDA) (4.98 g; 12.82 mmol) was suspended in chloroform (150 ml) and stirred at room temperature. Fuming HNO_3 >90% (50 ml) was added dropwise over a time period of 20 min. The PDA started to dissolve immediately. The reaction mixture was heated and refluxed overnight. After cooling to room temperature, the mixture was poured in 500 ml of water. The precipitate was filtered and washed with water until the filtrate reached a pH-value of approximately 7.

The crude orange/red product was dried under vacuum. Since the product is very weakly soluble it could not be purified by silica gel column or recrystallisation. Also, sublimation was tried, but the NMR showed, that the product was destroyed. The NMR shows the 1,7-isomer as well as the 1,6-isomer. Separation of those was not possible.

Yield (crude product): 7.18 g (81%)

^{1}H NMR (300 MHz, DMSO-d6, δ in ppm): 9.12 (s, 2H), 9.02 (s, 2H), 8,73 (d, *J*=8.49 Hz, 2H), 8.67 (d, *J*=8.49 Hz, 2H), 8.38 (d, *J*=8.88 Hz, 4H).

IR (cm^{-1}): 3064, 1774, 1742, 1599, 1538 (NO2),1401, 1367, 1340, 1305 (NO2), 1238, 1151, 1056, 808, 734,706, 565

3.4 Synthesis of mono Boc protected diamine

3.4.1 *tert*-butyl(4-aminophenyl)carbamate

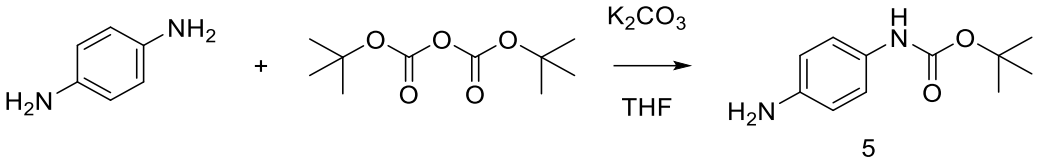

Scheme 3: preparation of Boc-protected phenylenediamine

A solution of Boc_2O (2.29 g; 10.4 mmol) in THF (5 ml) was added dropwise to a solution of phenylenediamine (3.32 g; 30.7 mmol) and K_2CO_3 (1.49 g; 10.7 mmol) in THF (25 ml) over a time period of 0.5 h. The mixture was stirred at room temperature overnight. TLC (CH/EtOAc 2/1) showed full conversion.
Then 70 ml of H_2O were added to the mixture and the product was extracted with 3x50 ml of CH_2Cl_2. The organic phases were combined, washed with brine, and dried over Na_2SO_4. The solvent was evaporated on a rotary evaporator.
Purification was done by silica gel chromatography with CH/EtOAc 2/1 as eluent.

Yield: 1.98 g (91%)

^{1}H NMR spectrum fits to literature[35]

^{1}H NMR (300 MHz, $CDCl_3$, δ in ppm): 7.12 (d, 2H, *J*=8.5 Hz), 6.62 (d, *J*=8.5 Hz, 2H), 6.15-6.35 (bs, 1H), 3.6-3.4 (bs, 2H), 1.75-1.2 (m, 9H).

3.5 Synthesis of perylene derivatives

3.5.1 di-tert-butyl((1,3,8,10-tetraoxo-1,3,8,10-tetrahydroanthra[2,1,9-def:6,5,10-d'e'f']diisoquinoline-2,9-diyl)bis(4,1-phenylene))dicarbamate

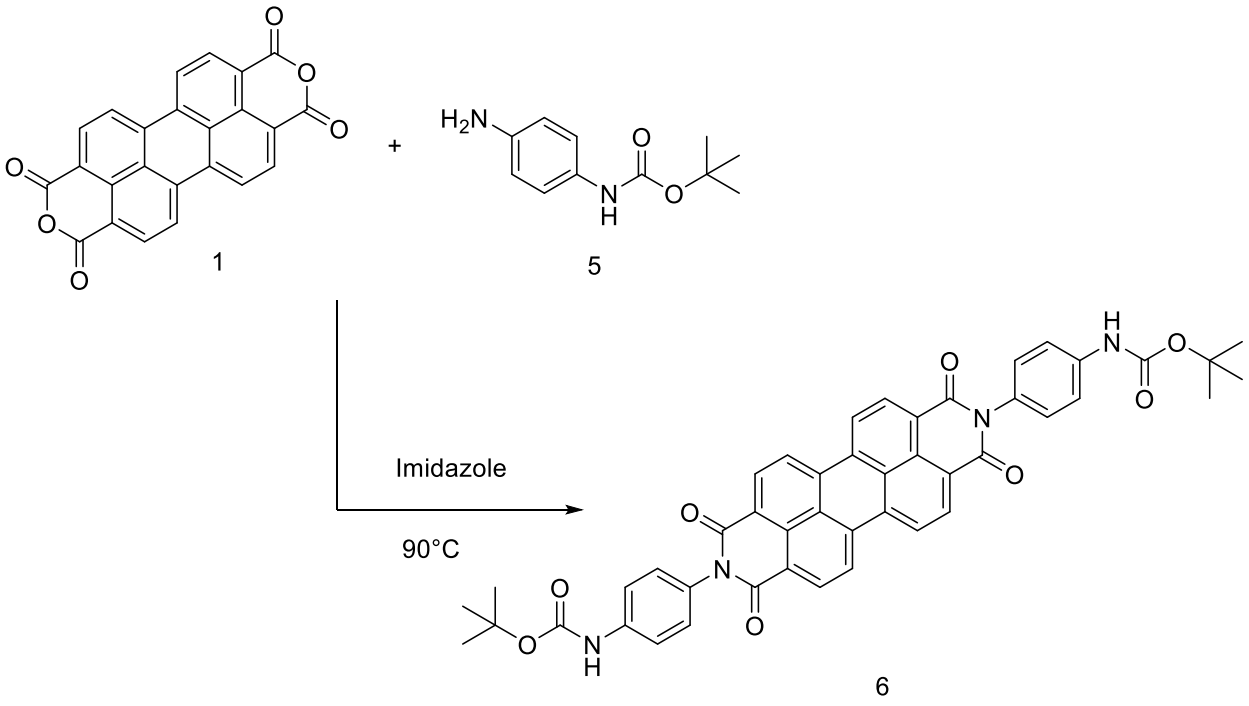

Scheme 4: preparation of PDI 6

PDA (0.463 g; 1.18 mmol) was mixed with *tert*-butyl(4-aminophenyl)carbamate (5) (0.538 g; 2.58 mmol) and 20 g of imidazole. Then the mixture was heated to 90°C. The imidazole started to melt, and a suspension was obtained. The reaction mixture was kept at this temperature for 24 h. After that period of time the heat was raised to 140°C and stirred for an additional 24 h. The reaction mixture turned dark red. After cooling to room temperature, the mixture was poured into 100 ml of water. The precipitate was filtered and washed with 5 % NaOH followed by water until the filtrate became neutral. The product was not soluble in common solvents. Therefore, only IR spectroscopy for characterization was carried out.

Yield: 613 mg (67%)

IR(cm^{-1}): 3345, 1695 (imide), 1654 (imide) , 1591, 1512, 1432, 1402, 1359, 1318, 1249, 1175, 1155, 1059, 971, 843, 808, 745, 659, 624, 532

3.5.2 2,9-di(tridecan-7-yl)anthra[2,1,9-def:6,5,10-d'e'f']diisoquinoline-1,3,8,10(2H,9H)-tetraone (PDI-8) and 9-(tridecan-7-yl)-1H-isochromeno[6',5',4':10,5,6]anthra[2,1,9-def]isoquinoline-1,3,8,10(9H)-tetraone (PDI-9)

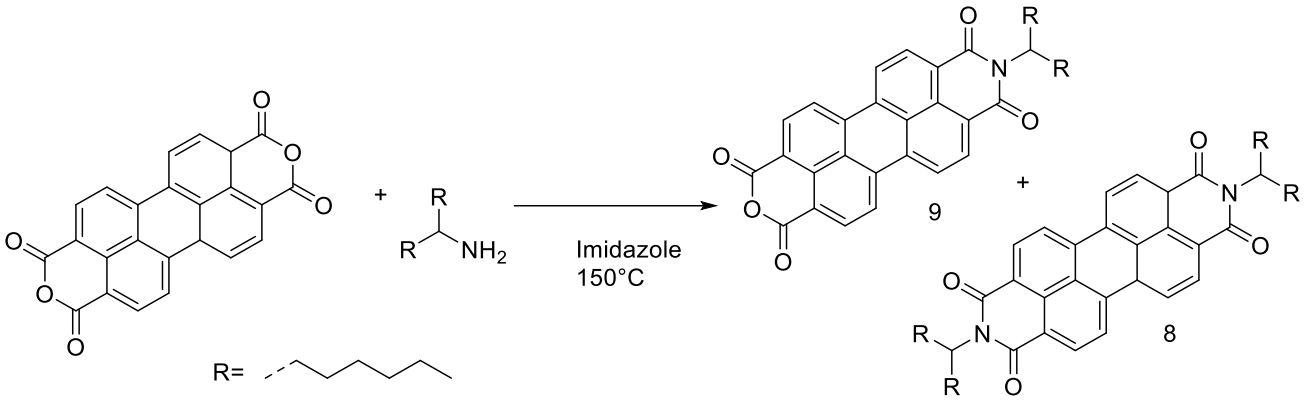

Scheme 5: Preparation of PDI 8

The synthesis was carried out similar to a description by Hu, Chen et al.[36]

PTCDA (4.371 g; 9.81 mmol), *N*-(1-hexylheptyl)amine (1.65 g; 9.6 mmol) and imidazole (40 g) were mixed and heated to 150°C. The imidazole melted immediately, and the mixture was stirred at 150°C over the weekend.

After cooling to room temperature 2 M HCl (250 ml) was added and stirred for 4 hours. The formed precipitate was filtered off with a paper filter and washed several times with CH_2Cl_2. Then the product was extracted from the filtrate with CH_2Cl_2. (500 ml). The organic layers were combined and washed with brine, dried over Na_2SO_4 and the solvent was evaporated on a rotary evaporator.

The crude product was purified by silica gel chromatography with DCM as eluent.

Yield: Monoimide: 0.032 g (0.6%)

Diimide: 1.4 g (20%)

Monomide: ^{1}H NMR spectrum fits to literature[36]

^{1}H NMR (300 MHz, $CDCl_3$, δ in ppm): 8.64-8.72 (m, 8H), 5.13-5.23 (m, 1H), 2.21-2.29 (m, 2H), 1.83-1.89 (m, 2H), 1.23-1.31 (m, 16H), 0.83 (t, 6H, *J*=6.5).

IR(cm^{-1}): 2919, 2850, 1765 (C=O anhy.), 1728 (C=O anhy.), 1695 (imide), 1652 (imide), 1588, 1574, 1504, 1453, 1401, 1352, 1311, 1243, 1120, 1011, 861, 806, 734

Diimide: ^{1}H NMR spectrum fits to literature[36]

^{1}H NMR (300 MHz, $CDCl_3$, δ in ppm): 8.64-8.72 (m, 8H), 5.13-5.23 (m, 2H), 2.21-2.29 (m, 4H), 1.83-1.89 (m, 4H), 1.23-1.31 (m, 32H), 0.83 (t, 12H, *J*=6.5).

IR(cm^{-1}): 2919, 2850, 1695 (imide), 1652 (imide), 1588, 1574, 1504, 1453, 1401, 1332, 1249, 1204, 1171, 1120, 1103, 960, 849, 806, 742, 620

3.5.3 9-(tridecan-7-yl)-1H-isochromeno[6',5',4':10,5,6]anthra[2,1,9-def]isoquinoline-1,3,8,10(9H)-tetraone (PDI-9)

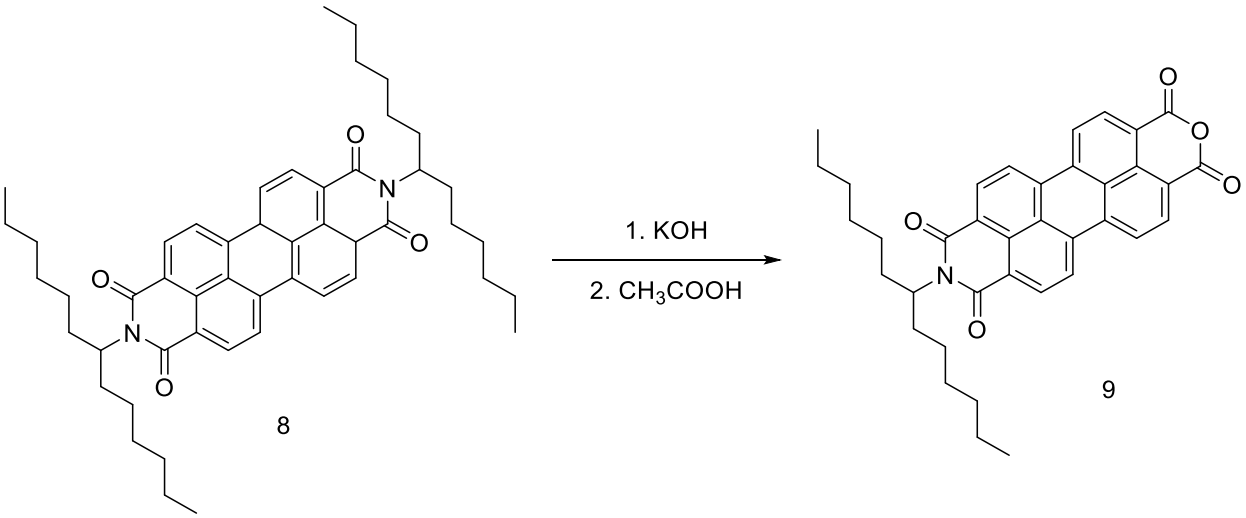

8 9

Scheme 6: Preparation of PDI 9

Perylenediimide 8 (0.959 g; 1.2 mmol), KOH (0.264 g) were dissolved in t-BuOH (35 ml) and heated to reflux for 1 h. After that time-period a mixture of 8 ml acetic acid and 32 ml of water was added.

The reaction mixture was stirred at reflux for 30 min and then at room temperature overnight.

The next day the product was extracted with 150 ml of DCM and washed several times with water. The organic layer was then dried over anhydrous Na_2SO_4. The solvent was evaporated and the crude product was cleaned by silica gel chromatography with DCM as eluent.

Yield: 303 mg (42%)

^{1}H NMR spectrum fits to literature[36]

^{1}H NMR (300 MHz, $CDCl_3$, δ in ppm): 8.64-8.72 (m, 8H), 5.13-5.23 (m, 1H), 2.21-2.29 (m, 2H), 1.83-1.89 (m, 2H), 1.23-1.31 (m, 16H), 0.83 (t, 6H, *J*=6.5).

IR(cm^{-1}): 2919, 2850, 1765 (C=O anhy.), 1728 (C=O anhy.), 1695 (imide), 1652 (imide), 1588, 1574, 1504, 1453, 1401, 1352, 1311, 1243, 1120, 1011, 861, 806, 734

3.5.4 tert-butyl (3-(1,3,8,10-tetraoxo-9-(tridecan-7-yl)-3,8,9,10-tetrahydroanthra[2,1,9-def:6,5,10-d'e'f']diisoquinolin-2(1H)-yl)propyl)carbamate (PDI-10)

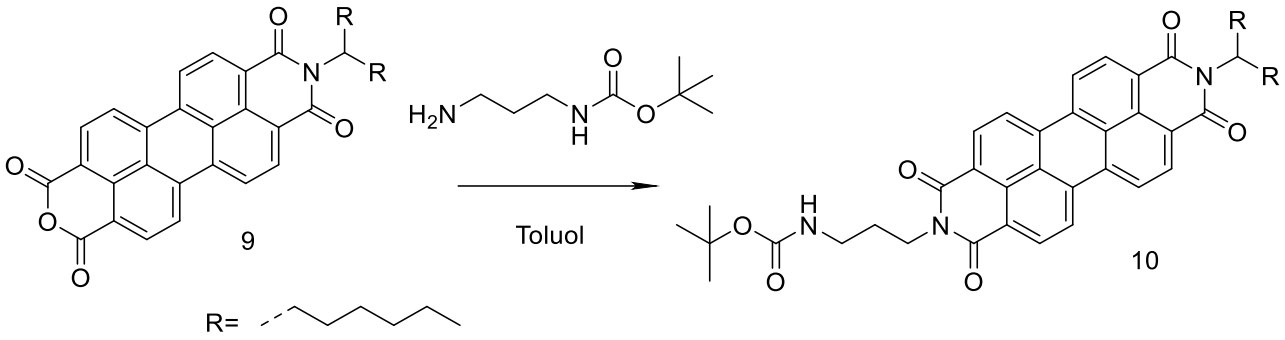

Scheme 7: preparation of PDI 10

Perylenemonoimide 9 (0.13 g;0.227 mmol) and tert-butyl N-(3-aminopropyl)carbamate (0.05 ml; 0.05 g; 0.281 mmol) were mixed with 15 ml toluene. The mixture was heated to 120°C under N_2 atmosphere. After 20 h TLC (DCM/MeOH 99/1) showed full conversion and the heat was removed.

After the mixture was cooled to room temperature the mixture was filtrated through a silica plug. All product stayed on the silica gel. Side products were removed by washing with pure DCM. The product was collected with a DCM/MeOH mixture of 9/1. The solvent was removed, and the residue was dissolved in a minimum of DCM and precipitated by adding MeOH. The precipitate was filtered off.

Yield: 0.094 g (57%)

^{1}H NMR spectrum fits to literature[37]

^{1}H NMR (300 MHz, $CDCl_3$, δ in ppm): 8.53-8.64 (m, 8H), 5.18-5.23 (m, 2H), 4.29 (t, 2H, *J*=6.3), 3.16-3.23 (m, 2H), 2.22-2.30 (m, 2H), 1.84-1.99 (m, 4H), 1.46 (s, 9H), 1.24-1.32 (m, 16H), 0.83 (t, 6H, *J*=6.5).

IR(cm^{-1}): 3392 (-NH); 2919, 2850, 1691(imide), 1648 (imide), 1590, 1502, 1434, 1401, 1334, 1247, 1169, 960, 849, 808, 744, 592

3.5.5 2-(3-aminopropyl)-9-(tridecan-7-yl)anthra[2,1,9-def:6,5,10-d'e'f']diisoquinoline-1,3,8,10(2H,9H)-tetraone (PDI-11)

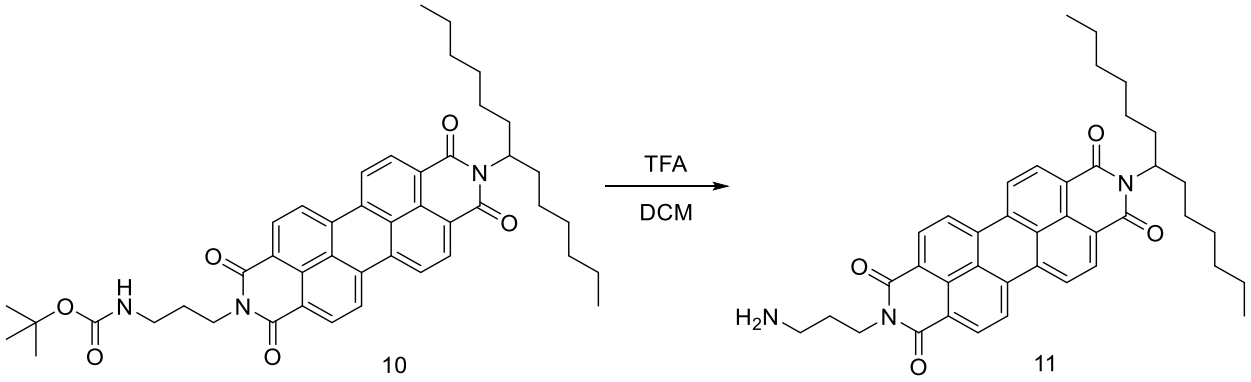

Scheme 8: preparation of PDI 11

Perylenediimide 10 (0.094 g; 0.128 mmol) was dissolved in DCM (4 ml). Then TFA (2 ml) was added. The mixture was stirred for 3.5 hours.
After full conversion (determined by TLC) 20 ml of a 10 wt% $NaHCO_3$ solution was added. The formed suspension was filtrated, and the red product was dried in vacuum.

Yield 0.080 g (98%)

^{1}H NMR spectrum fits to literature[37]

^{1}H NMR (300 MHz, $CDCl_3$, δ in ppm): 8.23-8.42 (m, 8H), 5.06-5.16 (m, 1H), 4.36-4.25 (br s, 2H), 2.9-3.0 (br s, 2H), 2.27-1.81 (br, 27H), 1.32-1.24 (br, 22H), 0.84 (t, 8H, *J*=6.5).

IR(cm^{-1}): 3538 (-NH_2) , 3300 (-NH_2), 2919, 2852, 1691(imide), 1648 (imide), 1590, 1502, 1434, 1401, 1334, 1247, 1169, 960, 849, 808, 744, 592

3.6 Synthesis of bay-substituted perylene derivatives

3.6.1 di-tert-butyl ((5,6,12,13-tetrakis(4-(tert-butyl)phenoxy)-1,3,8,10-tetraoxo-1,3,8,10-tetrahydroanthra[2,1,9-def:6,5,10-d'e'f']diisoquinoline-2,9-diyl)bis(propane-3,1-diyl))dicarbamate (PDI-13)

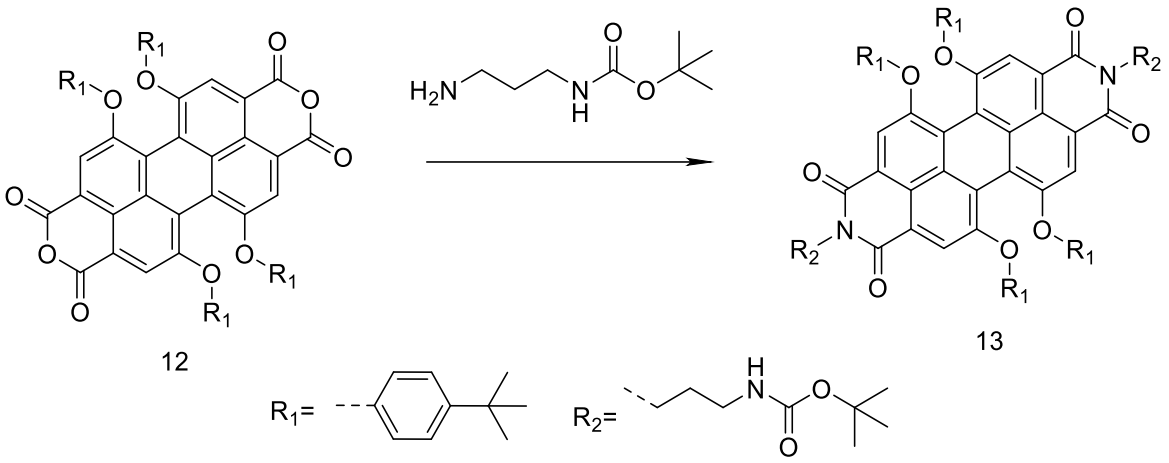

Scheme 9: preparation of PDI 13

Perylenedianhydride 12 (0.501 g; 0.509 mmol) and tert-butyl N-(3-aminopropyl)carbamate (0.220 ml; 0.22 g; 1.49 mmol) were mixed with toluene (50 ml). The mixture was heated to 120°C under N_2 atmosphere. After 24 h the reaction mixture was cooled down to room temperature and the solvent was evaporated. The crude product was purified by silica gel chromatography. The column was first eluted with pure DCM to separate side products and unreacted starting material. Then a mixture of DCM/MeOH 99/1 was applied. Due to the fact, that structurally very similar side products did form, the separation was not successful. Only a mixture of probably di-, tri-, and tetrasubstituted product could be obtained.

Yield (crude product): 0.36 g (55%)

The sample for the NMR spectroscopy was obtained by preparative TLC.
20 mg of the mixture were dissolved in a minimum of CH_2Cl_2. A line was spotted on the preparative TLC plate and it was eluted with DCM/MeOH 99/1.

^{1}H NMR spectrum fits to literature[38]. The shifts of the peaks fit good. The integrals however are not reliable since peaks are overlayed by impurities.

^{1}H NMR (300 MHz, $CDCl_3$, δ in ppm): 8.22 (s, 4H), 7.22-7.26 (m, 8H), 6.81-6.84 (m, 8H), 5.12 (br s, 2H), 4.2 (t, 4H, *J*=6.5), 3.12 (br s, 4H), 1.87-1.89 (m, 7H), 1.41(s, 25H), 1.29 (s, 48H).

IR(cm^{-1}): 3384 (-NH), 2956, 2862, 1693 (imide), 1652 (imide), 1584, 1500, 1434, 1406, 1346, 1268, 1212, 1167, 1108, 1013, 939, 877, 832, 803, 746, 551

3.6.2 2,9-bis(3-aminopropyl)-5,6,12,13-tetrakis(4-(tert-butyl)phenoxy)anthra[2,1,9-def:6,5,10-d'e'f']diisoquinoline-1,3,8,10(2H,9H)-tetraone (PDI-14)

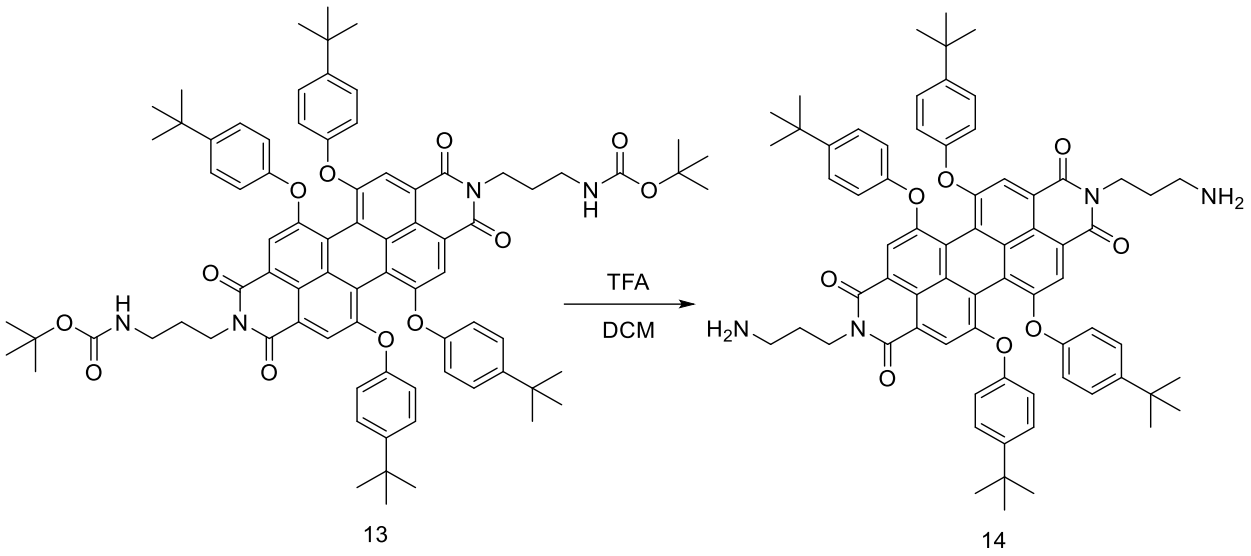

Scheme 10: preparation of PDI 14

Perylenediimide 13 (0.3 g; 0.23 mmol) was dissolved in 96 ml of DCM. Then with a syringe slowly TFA (2.8 ml) was added, and the mixture was stirred at room temperature for 4 h. The color changed from red to deep purple.

The reaction was quenched with saturated aqueous $NaHCO_3$ (2x50 ml) and then washed with water (2x100 ml). The organic layer was dried over Na_2SO_4 and the solvent was then removed with a rotary evaporator.

The residue was dissolved in a minimum amount of MeOH and tried to precipitate with water. Since no precipitate did form, $KHCO_3$ was added until the product did precipitate. The precipitate was filtered off, washed with water, and dried under vacuum.

Yield (crude product): 0.12 g (47%)

^{1}H NMR spectrum agrees reasonable with literature[39]

^{1}H NMR (300 MHz, $CDCl_3$, δ in ppm): 8.22 (s, 4H), 7.22-7.26 (m, 8H+solvent), 6.81-6.84 (m, 8H), 4.18-4.27 (m, 4H,), 2.72-2.73 (m, 4H), 1.80-1.88 (m, 4H), 1.29 (s, 36H + grease).

IR(cm^{-1}): 2956, 2862, 1693 (imide), 1652 (imide), 1584, 1500, 1434, 1406, 1346, 1268, 1212, 1167, 1108, 1013, 877, 832, 803, 746, 551

3.7 Perylene anhydrides as curing agents

General procedure:

The corresponding epoxide and anhydride were weight into a vial. As catalyst a stock solution of Et_3N or dimethylaniline (DMA) in, either dimethylacetamide (DMAc) or chlorobenzene, was added. The usual amount of catalyst was 3 mol% relative to anhydride. The closed vial was heated to temperatures between 120-200°C, usually overnight. If the reaction mixture did not solidify, the solvent was evaporated until a solid residue could be obtained. Typically, the molar ratio of anhydride to epoxy groups was between 1/1-1/2.

An overview of the exact reaction conditions (which epoxide was reacted with which anhydride, the type of solvent, temperature and catalyst) is shown in Table 1.

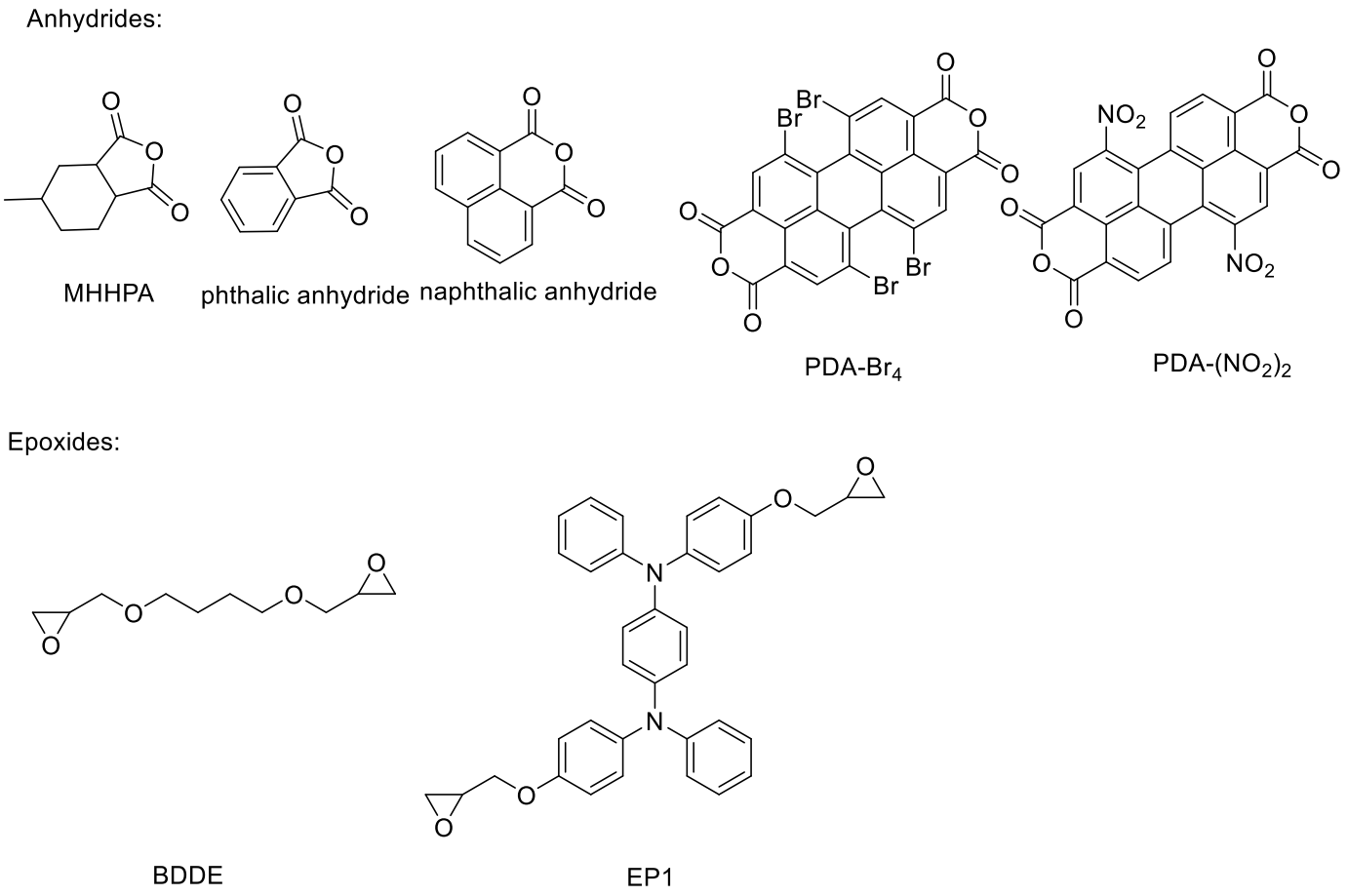

Figure 12: Abbreviations and structures of anhydrides and epoxides used

Table 1: reaction conditions with anhydrides as curing agents

	type of anhydride	amount anhydride [mmol]	mass anhydride [mg]	type of epoxide	amount epoxide [mmol]	mass epoxide [mg]	ratio anhydride/epoxide	solvent	amount of solvent [ml]	type of catalyst	reaction temp. [°C]
1	PDA-Br4	0.06	45	BDDE	0.25	50	1/4	DMAc	0.1	Et3N	170
2	PDA-Br4	0.04	31	BDDE	0.11	22	1 /2	DMAc	0.1	Et3N	110
3	PDA-(NO2)2	0.06	30	BDDE	0.15	31	1/ 2	DMAc	0.1	Et3N	180
4	PDA-(NO2)2	0.05	26	EP1	0.06	31	1/ 1	DMAc	0.1	Et3N	160
5	MHHPA	8.60	1447	BDDE	5.02	1015	1 /1	-	-	DMA	160
6	MHHPA	8.38	1409	BDDE	5.00	1011	1 /1	-	-	Et3N	160
7	MHHPA	0.29	48	EP1	0.17	92	1 /1.1	chlorobenzene	0.2	DMA	160
8	PMI-9	0.07	42	BDDE	0.05	10	1 /1.1	chlorobenzene	0.2	Et3N	180
9	Phthalic anhydride	0.34	51	BDDE	0.22	45	1 /1.1	chlorobenzene	0.1	Et3N	180
10	Phthalic anhydride	0.34	50	BDDE	0.22	45	1 /1.1	chlorobenzene	0.1	DMA	180
11	Naphthalic anhydride	0.35	69	BDDE	0.27	55	1 /1.1	chlorobenzene	0.2	Et3N	180
12	Naphthalic anhydride	0.35	70	BDDE	0.25	45	1 /1.1	chlorobenzene	0.2	DMA	180

3.8 Polymerization with amine-functionalized perylenes

General procedure:

Epoxide and amine functionalized perylene were weight into a vial and chlorobenzene was added. The molar ratio of epoxy groups to amine groups was 2/1 if not stated otherwise. Typically, 10mg of amine-functionalized perylene with the corresponding amount of epoxide, were dissolved in 0.1 ml chlorobenzene. The mixture was heated to 120°C and left overnight.

Table 2: reaction conditions for amine curing

type of amine	Amount amine [mmol]	mass amine [mg]	type of epoxide	Amount epoxide [mmol]	mass epoxide [mg]	ratio amine groups/ epoxide groups	solvent	amount of solvent [ml]	reaction temp. [°C]
PDI-11	0.017	11	BDDE	0.017	3.4	1/2	Chlorob-enzene	0.1	120
PDI-11	0.017	11	EP1	0.018	10	1 /2	Chlorob-enzene	0.1	120
PDI-14	0.03	34	EP1	0.054	30	1/ 2	Chlorob-enzene	0.1	150

3.7 Organic photovoltaics

3.7.1 Cell fabrication

Solar cells were built with an inverted design consisting of the following layers: glass substrate-cathode-ETL-active layer-HTL-anode. As cathode material ITO was used. The electron transport layer (ETL) consisted of ZnO and the hole transport layer (HTL) of MoO_3. As anode silver was used. As active layer polymer **EP1PDI-11** as single active material and **BDDEPDI-11 / PBDB-T** as bulk heterojunction material was used.

The following cells were prepared:

- Glass / ITO / ZnO / EP1PDI-11 / MoO_3 / Ag
- Glass / ITO / ZnO / BDDEPDI-11 / PBDB-T / MoO_3 / Ag
- Glass / ITO / ZnO / BDDEPDI-11/ MoO_3 / Ag
- Glass / ITO / ZnO / PBDB-T / MoO_3 / Ag

Prestructured glass-ITO substrates were purchased from Luminescence technology corp. All substrates were precleaned with acetone and then with iso-butanol in an ultrasonic bath at 40°C for 40 minutes. For removal of the remaining organic compounds and to obtain a more polar surface, the substrates were etched with a Femto oxygen plasma etcher from Diener Electronics for three minutes. The cleaned substrates were then transferred into the glove box.

The ZnO precursor solution for the electron transport layer was prepared by dissolving zinc acetate dihydrate (0.5 g $Zn(CH_3COO)_2 \cdot 2H_2O$) in 2-methoxyethanol (5 ml) using ethanolamine (150 µl) as stabilizer. The solution then was stirred at ambient conditions for a day. Afterwards the precursor was stored in the glovebox.

To form the ZnO layer on the substrates, the solution was filtered using a 0.45 µm PTFE filter. Subsequently, 35 µl precursor solution was coated on the cleaned and plasma etched substrates using a one-step spincoating process with the parameters given in Table 3.

Table 3: Spin coating parameters for the ZnO layer

Speed [rpm]	**Acceleration [rpm/s]**	**Time [s]**
4000	2000	30

After the spincoating process, the substrates were annealed on a heating plate at 150°C for 15 min at ambient atmosphere to form a smooth ZnO layer.

3.7.2 Preparation of the active layer

The active layer was prepared by dissolving the polymers in chlorobenzene.
For the cell, using only **EP1PDI-11** as single component active material, the polymer was weight into the vial and dissolved in chlorobenzene at 90°C over night. A concentration of 20mg/ml was achieved.

For the devices with a blend of **BDDEPDI-11 / PBDB-T** the polymers were weight into different vials and transferred into the glovebox. First BDDEPDI-11 was dissolved in chlorobenzene. To obtain homogeneous smooth films on the substrate the solution was filtered through an 0.45 µm PTFE filter. Then the solution was transferred into the vial with PBDB-T in it which was dissolved at 60°C over night. A concentration of 10mg/ml of each polymer was achieved.

Also, cells with only PBDB-T and only BDDEPDI-11 as active layer were produced. For the spincoating solutions a concentration of 20mg/ml was prepared.

Before the spin coating process the solution was heated to 60°C to prevent precipitation of the solution.
The thin films were prepared by a two step spin coating process:

- Step 1: x rpm; 500 rpm/s for 60s
- Step 2: 4000 rpm; 4000 rpm/s for 5s

The rotation speed in step 1 was varied from 1000 to 4000 rpm, to achieve different layer thicknesses. All cells with EP1PDI-11 were annealed. Two substrates were prepared at each spincoating speed. One of each was annealed at 150°C and one at 200°C for 15 minutes.
For the BDDEPDI-11 / PBDB-T only one cell at each spincoating speed was annealed at 150°C for 15min the others were used without annealing.

3.7.3 Preparation of the HTL and Anode

The hole transport layer (MoO_3) and the anode (Ag) were prepared by evaporation deposition. Therefore, the cells were placed into a mask creating six well defined areas for six solar cells per substrate.

In the first step MoO_3 was thermally evaporated with a rate of 0.1-0.2 Å/s giving a 10 nm layer. In the second step Ag was thermally evaporated with a rate of 0.4-1.6 Å/s giving a layer thickness of 100nm.

All evaporation processes took place in a high vacuum of approximately 10^{-5} mbar.

3.7.4 J-V characteristics

To characterize organic solar cells, J-V curves under illuminated and dark conditions are recorded. An example of such a curve is given in Figure 13.

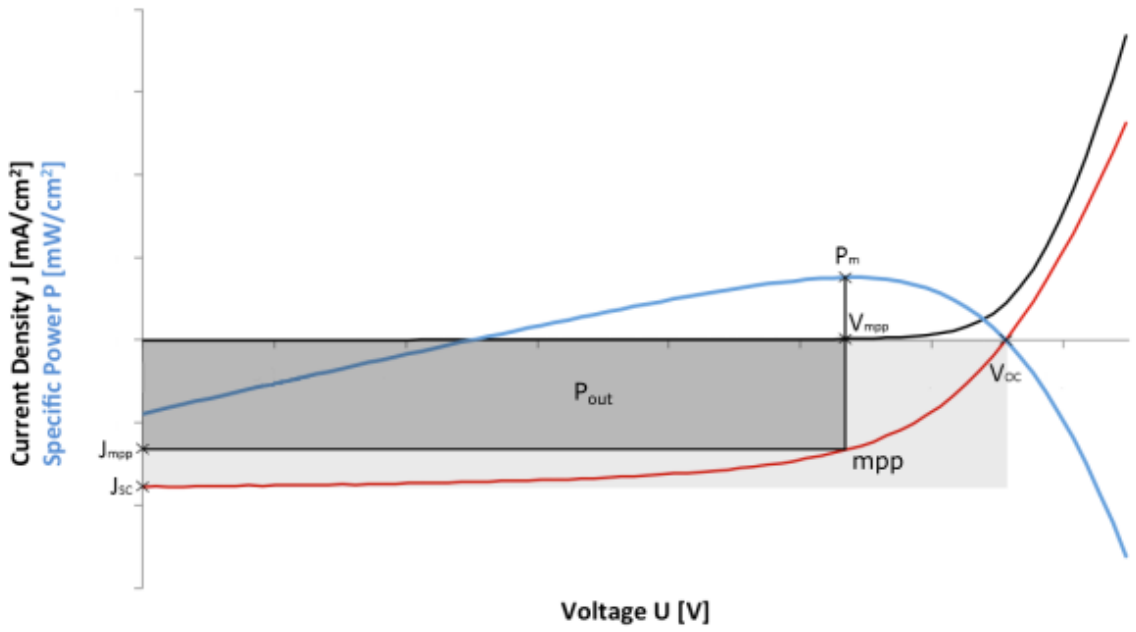

Figure 13: General J-V characteristics with all important parameters

As it can be seen, the gray rectangle describes the maximum power output of the solar cell. P_{out} can be described with the maximum power point (mpp). At this point, the product of current density and voltage has its maximum.

Other important parameters to mention are the open circuit voltage (**V_{oc}**), the short circuit density (**J_{sc}**), the fill factor (**FF**) and the power conversion efficiency (**PCE**).[40]

- **V_{oc}**: is the voltage at which the current density output is zero. It is dependent on the HOMO level of the donor and the LUMO level of the acceptor. Where the effective bandgap (Eg,eff) defines the theoretical limit.

- **J_{sc}**: is the measured current when the externally applied voltage is zero. It is representative for the number of charge carriers generated and transported to the electrodes. Improving of the carrier mobility, absorption coefficients, band gap difference and reducing of phase separation leads to improvement of Jsc.

- **FF:** is a factor describing the shape of a J-V curve and can be calculated by

$$FF = \frac{P_m}{J_{sc}V_{oc}} = \frac{J_{mpp}V_{mpp}}{J_{sc}V_{oc}}$$

where J_{mpp} and V_{mpp} is the current density and voltage at maximum power point. It therefore relates the theoretical achievable power output to the real power output.

- **PCE:** gives the efficiency of a solar cell and can be calculated by

$$PCE = \frac{P_m}{P_{in}} = \frac{V_{oc}J_{sc}FF}{P_{in}}$$

where P_{in} is the incoming power from the light source. Therefore, the PCE is the ratio of the generated electrical power and the incoming energy of the sun light.

4. Results and Discussion

4.1 Nitrated perylene anhydrides

The nitration reaction was carried out according to a description of Hao, Jiang et al. [41] However, they only described a method for obtaining a mixture of mono- and di-nitrated perylene anhydride.

The carried-out reactions have shown, that when the reaction is done at room temperature, the main product is the mono-nitrated perylene tetracarboxylic anhydride (PDA-(NO_2)).

When carrying out the reaction at elevated temperatures, it could be seen, that the main product is the di-nitrated perylene tetracarboxylic anhydride (PDA-(NO_2)$_2$) consisting of a mixture of the 1,6- and 1,7-isomer.

This is supported by the fact, that the products of the two reactions show a different color and compared to the mono-nitrated product, the di-nitrated product is better soluble. In all reported studies dealing with this compound, the nitrated perylene anhydride was reacted further to the perylene diimide and purified after this step because of better solubility and processability. This has not been done in this work since the desired product was the anhydride.

The UV-Vis spectra were compared with Tsai, Chang et al.[42], although they measured the nitrated perylene diimide, the nitrated perylene anhydride compound showed similar absorption behavior.

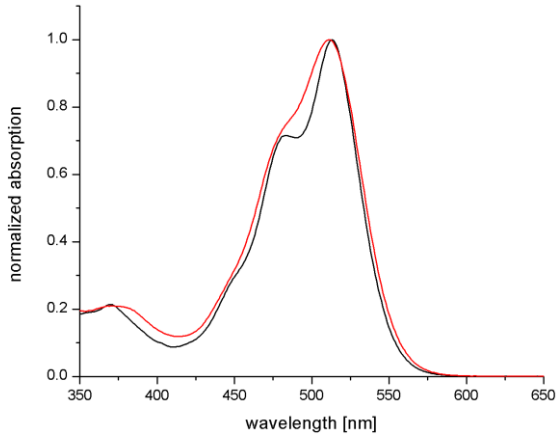

Figure 14: UV-Vis spectra of mono- (black) and di- (red) nitrated perylene anhydride in CH_2Cl_2

Figure 14 shows the UV-Vis spectrum of the mono- and di-nitrated perylene anhydride. The di-nitrated derivative has a maximum at 515 nm whereas the mono-nitrated compound has a maximum at 518 nm. Those peaks can be assigned to the π-π* transitions of the perylene core. Furthermore, the mono-nitrated perylene shows a strong shoulder at approximately 480 nm. This shoulder is smaller for the di-nitrated perylene. All those observations are in agreement with the reported observations of Tsai, Chang et al.[42]

Since the solubility of this compound is very poor, purification of the products was not possible and therefore not done in this work. Several attempts were made to purify the crude mixture, without reacting the dianhydride to the diimide but all tries failed.

4.2 Synthesis of PDI 11

Scheme 11 shows the synthetic route towards PDI 11.

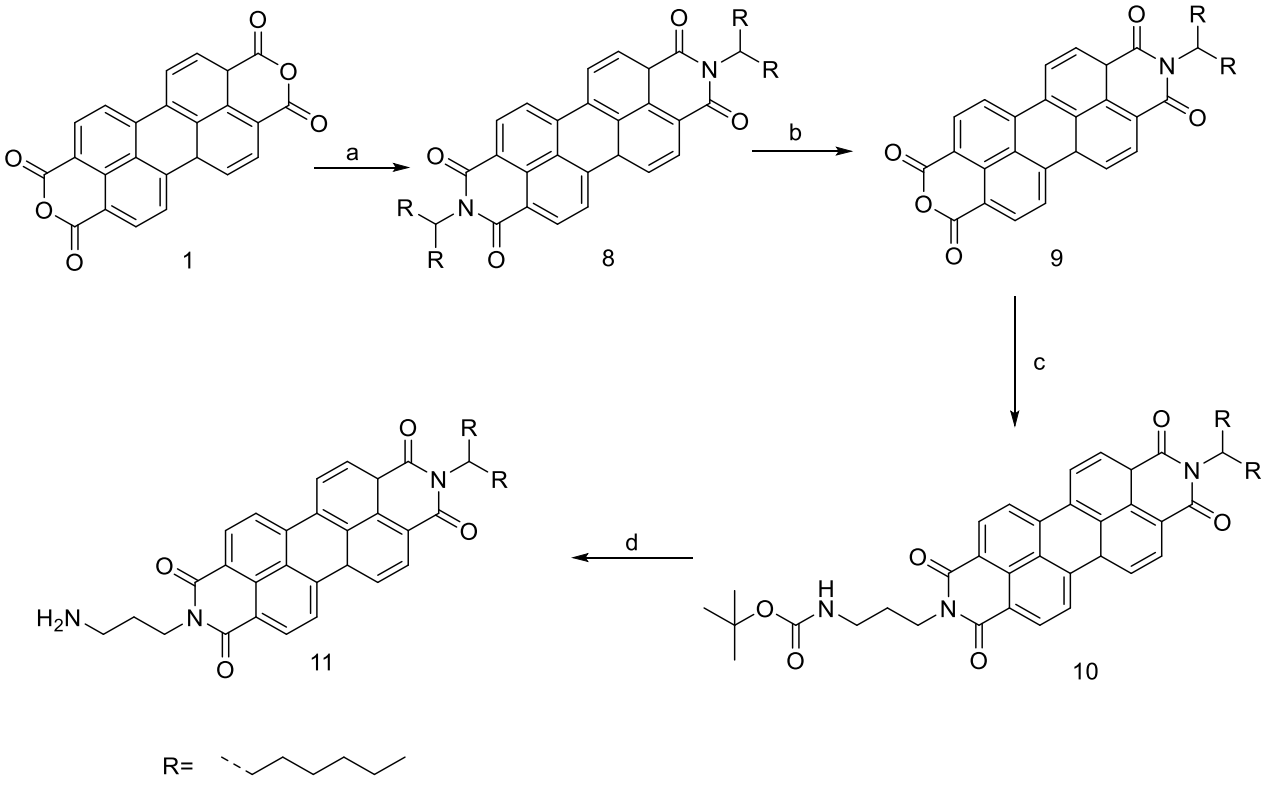

Scheme 11: Synthesis of PDI 11-(a) N-(1-hexylheptyl)amine, imidazole, 150°C (b) 1.KOH, 2.acetic acid (c) tert-butyl N-(3-aminopropyl)carbamate, toluene, 120°C (d) TFA, DCM

In the first step the perylene dianhydride (**1**) was reacted with a primary amine to give diimide **8**. This was then selectively hydrolyzed to give the desired mono-imide (**9**).
To that end, KOH was used to open the imide and split off the amine. First a carboxylic acid was produced and the ring closure to the anhydride was possible in hot acetic acid. It was expected that the amount of KOH was crucial to selectively obtain the mono-imide (**9**). However, we discovered that the mono-imide formation was in fact favored and no dianhydride (**1**) was obtained, regardless of the amount of KOH. This observation was also described in literature.[36] One step conversion from **1** to **9** was not possible in reasonable yields, as di-imide (**8**) was formed, regardless the amount of amine used. This could be explained by the fact that the solubility of the mono-imide increases drastically compared to the anhydride.
To obtain the amine functionalized perylene (**10**), a mono Boc protected diamine was used. The protection group was necessary to prevent a polymerization reaction to give a polyimide. The procedure described was adopted from literature.[38]
The reaction worked without any complications and NMR spectra fit to literature.[37]
The last step was the removal of the Boc-group of the amine group, which was performed according to the standard procedure with TFA in DCM. Compound **11** was obtained in good yields. Purification was not necessary. The IR spectrum shows a broad peak at about 3500 cm^{-1} with a shoulder at 3300 cm^{-1}. It is assumed that this peak corresponds to the NH_2 group, although according to literature two discrete peaks should be observed for primary amine groups. It is assumed that some water is still bound to the amine group and therefore a broadening of the peak is observed. Furthermore, the disappearance of the $C(CH_3)_3$- deformation mode of the Boc group, which should be at around 1200 cm^{-1} could not be observed due to overlapping peaks.[43] Also the disappearance of the C=O peak of the Boc group, at around 1700 cm^{-1} could not be seen, due to the overlap of the imide peak.[44]

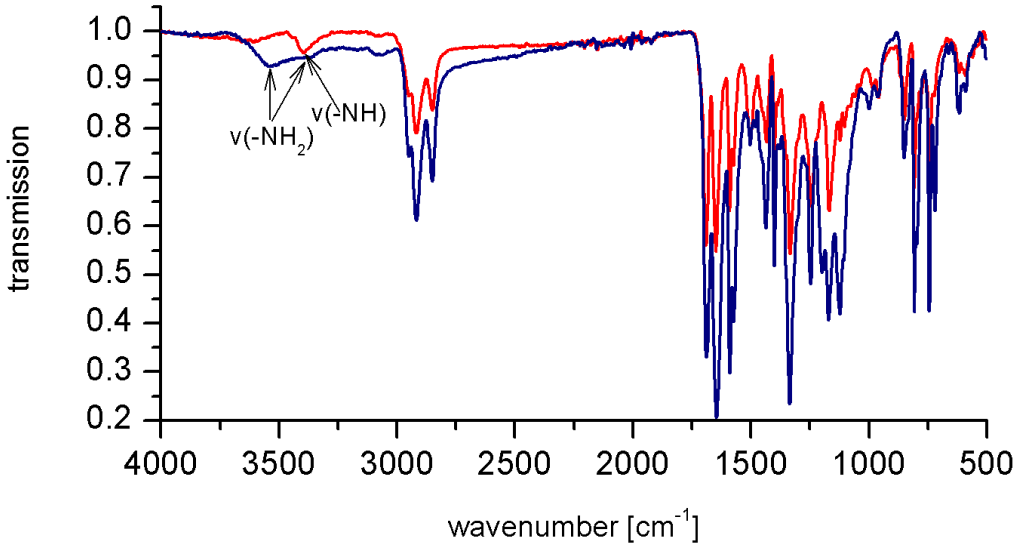

Figure 15: IR of PDI-10 (red) and PDI-11 (blue)

NMR spectroscopy (Figure 16) supports the theory of the interfering water, because the peak at about 2 ppm shows a water overlay, showing interactions of the amine group with water. All other peaks correspond to the literature values.[37] The integrals of the peaks at 1.25 ppm and 0.84 ppm do not correspond to the desired values due to some non-volatile higher alkanes from the used solvents.

To make sure, that the free amine is present, an NMR sample was mixed with a drop of TFA.

TFA is often used to simplify ^{1}H NMR spectra as it can exchange its proton with exchangeable protons in the sample. Due to high exchange rates, usually all exchangeable protons result in one broad peak shifted between the shift of the pure TFA and the shift of the exchangeable protons.[45] In the spectrum of compound **11** the peak at 2 ppm splits in two peaks. A new peak appeared at around 6 ppm, corresponding to the TFA/water protons. Therefore, the peaks at 2 ppm could be properly assigned.

With the 2D COSY spectrum, the peak at 7.5 ppm could be identified as the NH_2 peak. Also indicating protonation of the NH_2 peak with TFA since it shifted from around 2 ppm to 7.5 ppm.

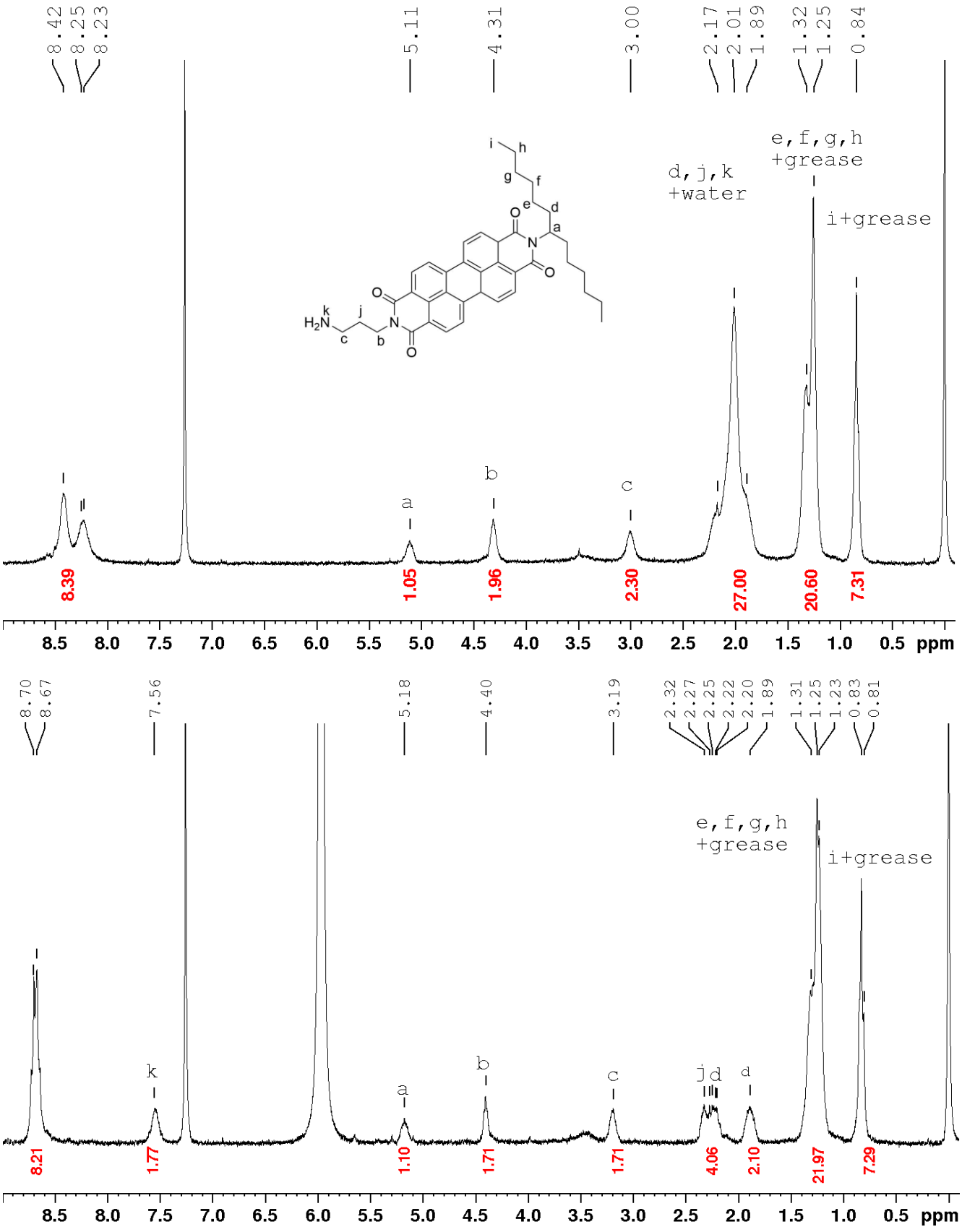

Figure 16: ^{1}H NMR of PDI 11 without (top) and with (bottom) TFA

4.3 Synthesis of PDI 14

Scheme 12 shows the synthetic route towards PDI14.

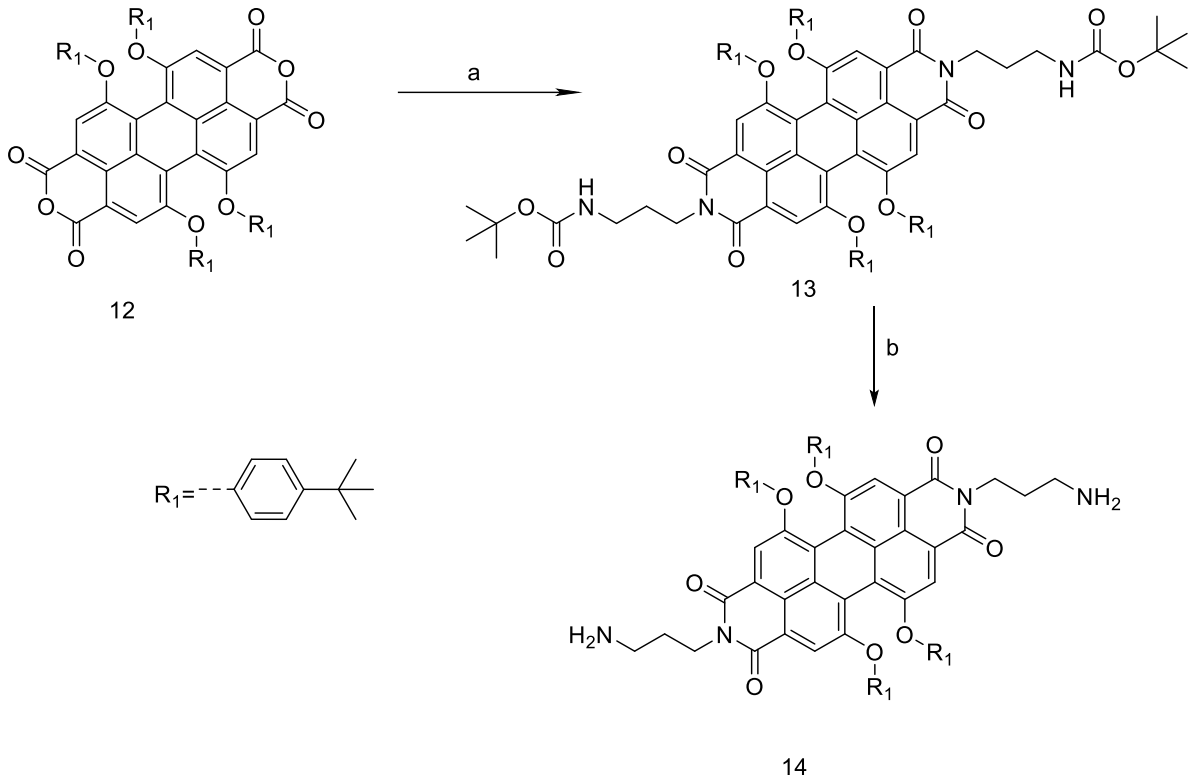

Scheme 12: Synthesis of PDI 14-(a) N-Boc-1,3-propanediamine, toluene, 120°C (b) TFA, DCM

PDA-12 was purchased from abcr in technical grade. TLC and NMR spectroscopy showed that many impurities were present. Nevertheless, the synthesis of PDA-12 to PDI-13 was performed without purification of PDA-12. It was assumed, that the more polar PDI-13 would be easier to purify with column chromatography. However, TLC showed that the different impurities (presumably di-, tri- and tetra bay-substituted perylene) also reacted to the diimide and had Rf values very close to each other. Separation by column chromatography was attempted but was not successful because only a separation of the starting material could be achieved, as shown in Figure 17.

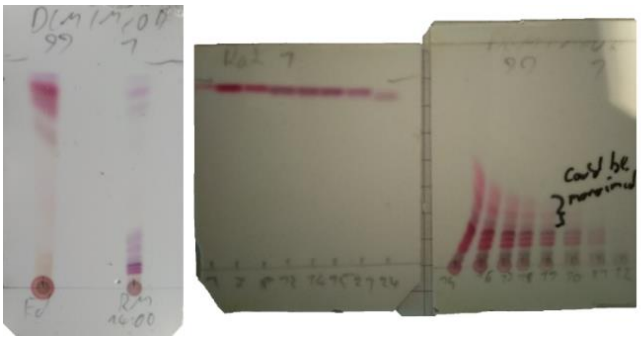

Figure 17: TLC of the reaction mixture (left) and the column (right) of PDI-13

Also recrystallization from methanol, as described in literature[38], was without success. With a preparative TLC, it was possible to obtain the cleanest sample of PDI-13. Impurities and non-volatile higher alkanes from the solvent were detectable in the NMR spectrum. However, since separation and clean up was not possible, deprotection of PDI-13 was done without further purification. Therefore, all further reactions with PDI-14 were performed with the crude mixture.

The IR spectrum of PDI-14 did not show the characteristic NH_2 group. This fact could not be explained. It is suspected that perhaps the signal of the NH_2 group is superimposed by the background and therefore lost.

The ^1H NMR spectrum, however, shows that the NH-group at 5.1 ppm disappeared. The NH_2 peak most likely appeared at approximately 1.7 ppm. Confirmation cannot be given since the peak is overlayed by impurities. In literature it is also described, that the NH_2 peak was not observed in ^1H NMR.[39]

Further the $-CH_3$ signal of the Boc protection group at 1.4 ppm is missing, and therefore shows that the deprotection was successful.

Also, TLC showed a great increase in polarity of the compound also indicating, that the primary amine did form.

4.4 Using peryleneanhydrides as curing agents for epoxy resins

In the following section different perylene carboxylic anhydrides have been investigated according to their ability of curing EP1 and BDDE.

To determine the optimal reaction conditions different reactions were carried out. The results are given below. All numbered reactions in the following section refer to the reactions given in Table 4.

Table 4: polymerization attempts with anhydrides

	type of anhydride	**Amount anhydride [mmol]**	**type of epoxide**	**Amount epoxide [mmol]**	**ratio anhydride/epoxide**	**solvent**	**type of catalyst**
1	PDA-Br4	0.06	BDDE	0.25	1/4	DMAc	Et3N
2	PDA-Br4	0.04	BDDE	0.11	1 /2	DMAc	Et3N
3	PDA-(NO2)2	0.06	BDDE	0.15	1/ 2	DMAc	Et3N
4	PDA-(NO2)2	0.05	EP1	0.06	1/ 1	DMAc	Et3N
5	MHHPA	8.60	BDDE	5.02	1 /1	-	DMA
6	MHHPA	8.38	BDDE	5.00	1 /1	-	Et3N
7	MHHPA	0.29	EP1	0.17	1 /1.1	chlorobenzene	DMA
8	PMI-9	0.07	BDDE	0.05	1 /1.1	chlorobenzene	Et3N
9	Phthalic anhydride	0.34	BDDE	0.22	1 /1.1	chlorobenzene	Et3N
10	Phthalic anhydride	0.34	BDDE	0.22	1 /1.1	chlorobenzene	DMA
11	Naphthalic anhydride	0.35	BDDE	0.27	1 /1.1	chlorobenzene	Et3N
12	Naphthalic anhydride	0.35	BDDE	0.25	1 /1.1	chlorobenzene	DMA

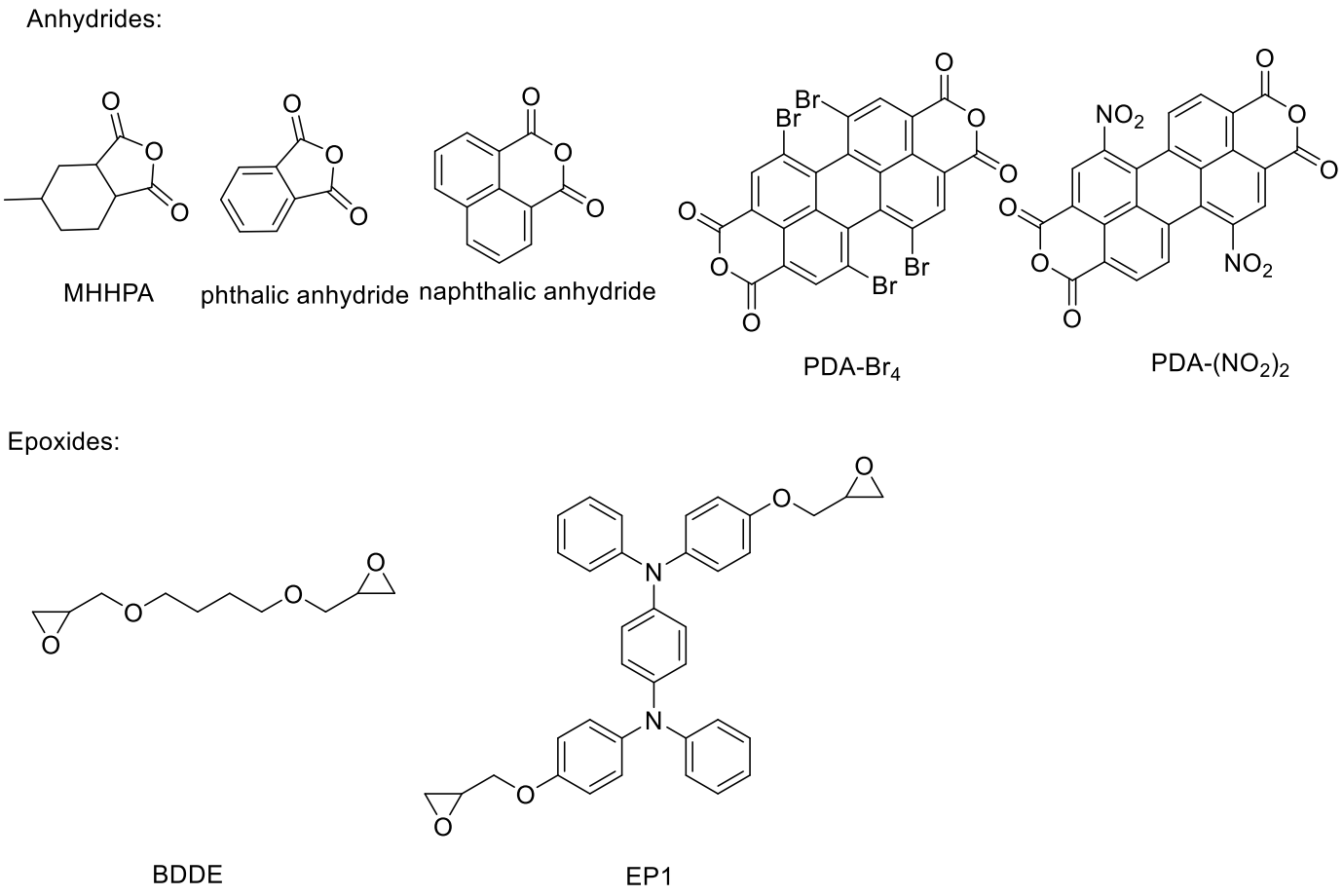

Figure 18: Abbreviations and structures of anhydrides and epoxides used

The first reaction attempts were carried out with PDA-Br_4. This model compound was chosen, because it is commercially available, and the bromine substituents increase the solubility of the PTCDA.

Reactions 1 and 2 differed by temperature (170°C and 110°C, respectively) and molar ratio (A/E 1/4 and 1/2, respectively). While reaction 1 formed an insoluble resin after evaporation of the solvent, this was not the case with reaction 2. Therefore, it can be concluded that a higher temperature was required to open the anhydride to allow the polymer reaction to take place. However, this observation and the fact that the solubility of the perylene derivatives was bad, also raised concerns about the possibility that only homopolymerization of the epoxide took place. This concern also is supported by the fact that reaction 1 had a 4-fold excess of epoxide. [46]

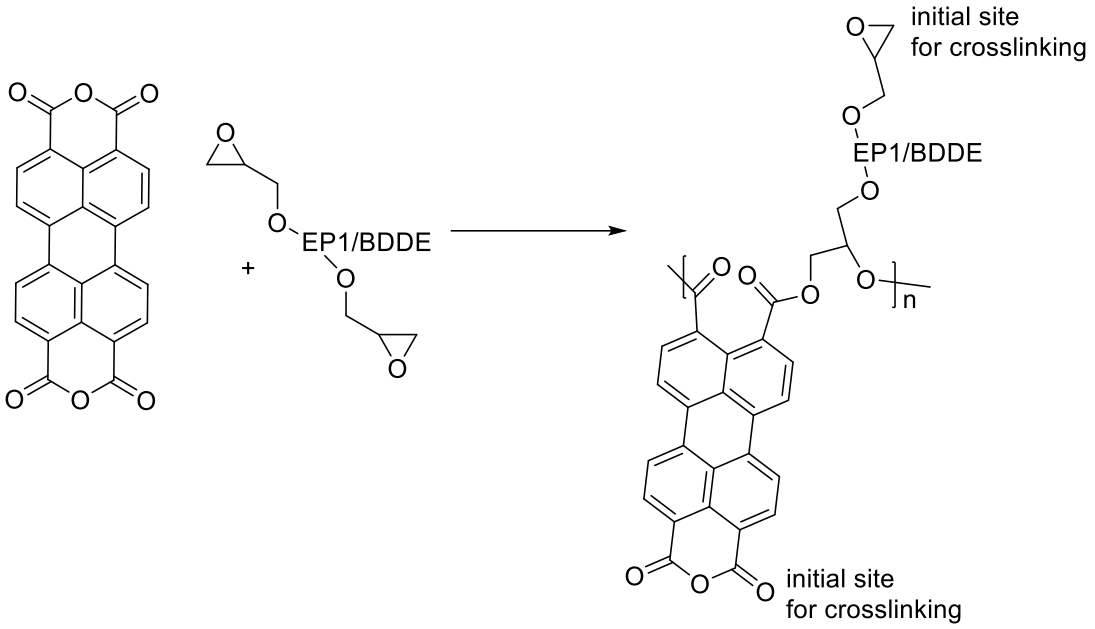

Figure 19: Theoretical polymeric structure for cured resins with perylene tetracarboxylic anhydride as curing agent. To simplify the structure only one anhydride and one epoxide per molecule was reacted

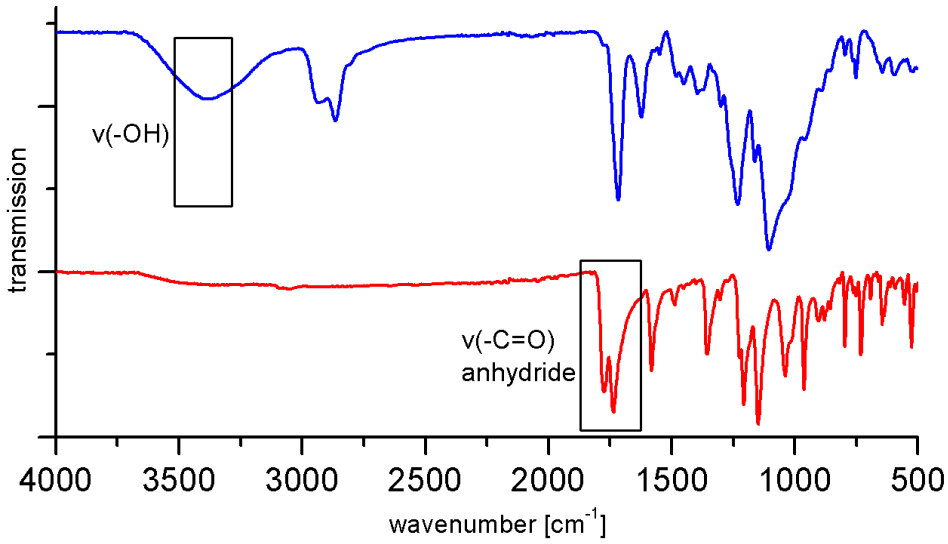

Figure 20: IR spectra of the product of reaction 1 (blue) and of the anhydride PDA-Br_4 (red)

IR-spectroscopy was used to investigate the insoluble residue.

Two characteristic anhydride peaks (1776 cm^{-1}, 1736 cm^{-1}) of the starting material are missing (Figure 20), which suggests that the reaction of the anhydride has taken place. A broad peak appeared at 3390 cm^{-1}, this peak corresponds to an OH group and the formation could not be explained at this time.[47] Thoughts were, that only a low degree of polymerization could be achieved, resulting in a large number of OH-groups. However, concerns also emerged that the anhydride was only hydrolyzed, and the free acid was present. This fact could indeed be confirmed with later reactions.

Subsequently, attempts were made to incorporate the nitrated perylene derivative (PDA-$(NO_2)_2$) into the polymer. On the one hand because the nitrated perylene should be a better electron acceptor for further applications and on the other hand because of its better solubility.[48]

Therefore, reactions 3 (180°C; A/E 1/2) and 4 (160°C; A/E 1/2) were carried out. Reactions 3 and 4 did not give much information about the polymerization itself, but one could clearly see that the nitro group was not stable.

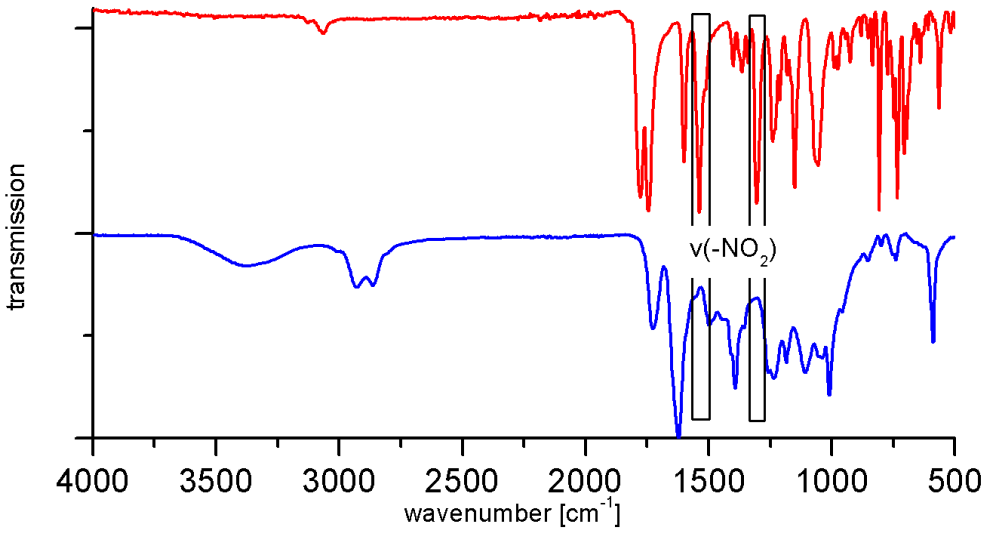

Figure 21: IR spectra of PDA-$(NO_2)_2$ (red) and of reaction 3 (blue)

Figure 21 shows the IR spectrum of the nitrated perylene and the reaction product of reaction 3. For the anhydride and hydroxy peak, the same applies as discussed before. However, the NO_2-peaks at 1538 cm^{-1} and 1306 cm^{-1} are missing, showing the reactivity of the NO_2 groups. It is known that nitrated perylenes are very reactive and can readily react at room temperature with nucleophiles. They are used as starting materials for a variety of compounds.[49]

Therefore, no further polymerization attempts with nitrated perylenes were carried out, due to the fact, that the exact reaction of the NO_2 group was unclear.

Because of uncertainties regarding the ability of peryleneanhydrides as curing agents and Et_3N and dimethylaniline as catalyst, polymerization reactions with a simpler anhydride were performed. (Figure 22)

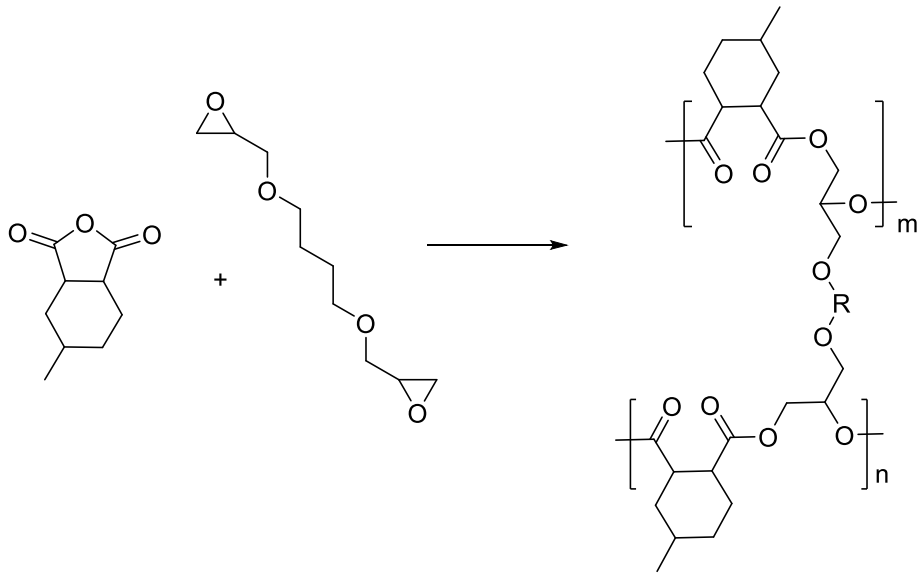

Figure 22: Polymerization of MHHPA with BDDE

MHHPA and BDDE are both liquid and therefore no solvent was needed. One reaction was done with dimethylaniline (reaction 5) and one was done with Et_3N (reaction 6), to see if polymerization at the given conditions in principle is possible. In both cases the A/E ratio was 1/1.

Reaction 5 started to get viscous after 35 min and was solid after 45min.

Reaction 6 solidified after 10 min in a very fast reaction. Therefore, Et_3N seems to be a better catalyst, by means of the reaction time, then dimethylaniline and both are capable of catalyzing the curing reaction for aliphatic anhydrides such as MHHPA.

Figure 23: Polymerization of BDDE and MHHPA with dimethylaniline (left) and ET_3N (right)

To see if the epoxy resin also solidifies when a solvent is present, the same reaction was carried out in chlorobenzene (reaction 7). Formation of a solid product was observed, and IR spectroscopy also confirms the formation of the polymer.

All polymerization attempts carried out with perylene tetracarboxylic anhydrides never solidified in solution, indicating that no crosslinked network did form. It was assumed that the perylene tetracarboxylic anhydride had to be more soluble to achieve a proper polymerization. Therefore, a better soluble perylene carboxylic anhydride PMI-9 was synthesized and used in further polymerization experiments. PMI-9 has only one anhydride group. The second anhydride was reacted to an imide with long bulky aliphatic chains. Those chains weaken the strong π-π stacking and increase the solubility of the compound drastically.
Although PMI-9 has only one anhydride group, cross-linked resins should still be formed because a bifunctional epoxide is used.

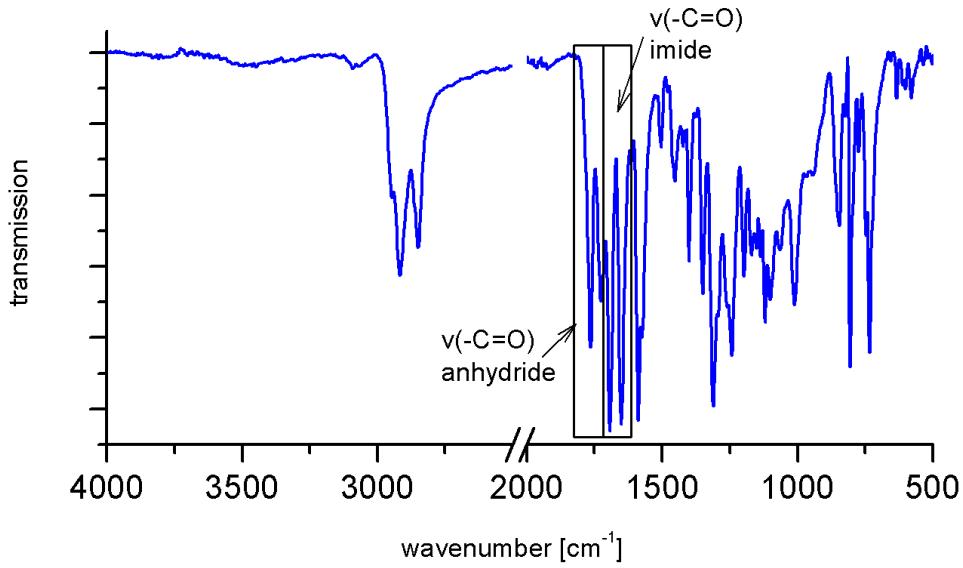

Figure 24: IR spectrum of reaction 8 after evaporation of solvent

When reacting PMI-9 and BDDE in chlorobenzene (reaction 8) no reaction took place also upon elongated time (24h). This can be seen in Figure 24, due to the fact, that the anhydride peaks at 1765 cm^{-1} and 1728 cm^{-1} could still be seen in IR spectrum.
The only major difference to the other polymerization attempts with perylene carboxylic anhydrides was that instead of DMAc chlorobenzene as solvent was used. This change in solvent unexpectedly showed that the anhydride is not reacting with the epoxide.

The reaction of the anhydride peak at the before mentioned polymerization experiments (reaction1-7) can be explained as follows.

The DMAc used was not absolute dry and had small amounts of water in it. Thus during the reaction, the anhydride was probably hydrolyzed, and a carboxylic acid was formed. Although carboxylic acids are also known curing agents for epoxy resins, it is assumed that because of the generally lower reactivity the formed carboxylic acid was also not able to react with the epoxide or that the homopolymerization of the epoxide is faster.

When comparing the IR spectra of the different polymerization attempts the theory of the formation of a carboxylic acid is supported.

Figure 25 shows the IR spectra of carried out polymerization attempts of perylene carboxylic anhydrides in DMAc (bottom) and successful polymerizations with simpler anhydrides (top).

It can be seen that for the successful polymerizations, there is either no OH-peak or one at approximately 3500 cm^{-1}, whereas for all attempts in DMAc a OH-peak can be observed at approximately 3300 cm^{-1}. The shift to smaller wavenumbers indicates that the OH-groups of the unsuccessful attempts correspond to a carboxylic acid. The peaks at approximately 1730 cm^{-1} correspond to either the C=O bond of the ester or the carboxylic acid.[50,51]

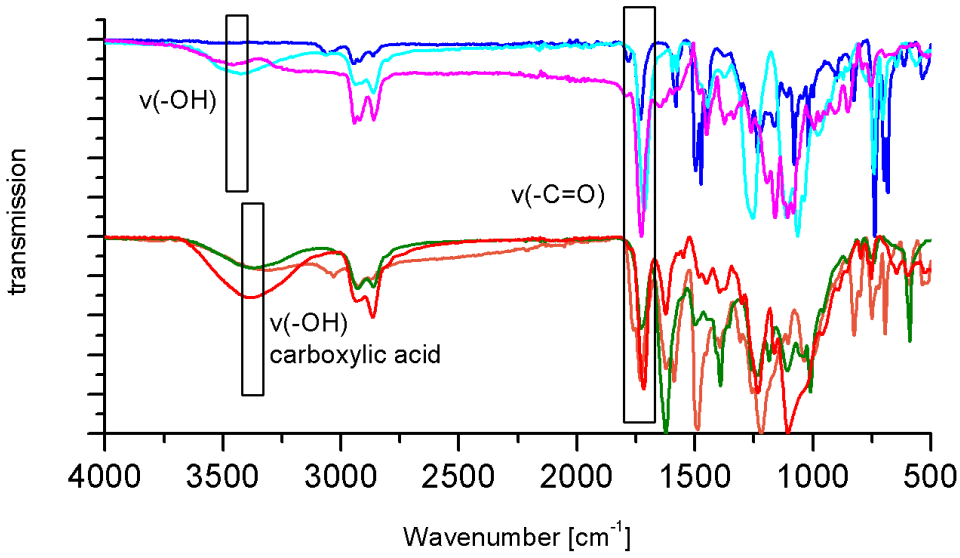

Figure 25:IR of polymerizations reaction 7 (blue), 10 (cyan), 5 (pink), 3 (green), 4 (orange), 1 (red)

All attempts using perylene carboxylic anhydrides as curing agent did not work. It was assumed that the stable six-membered ring structure of the anhydride might be too unreactive for the reaction using tertiary amines as catalyst. In order to prove this assumption, a chemical similar anhydride, naphthalic carboxylic anhydride was chosen. Polymerization reactions of BDDE with naphthalic carboxylic anhydride (reactions 11 and 12) were attempted. The IR spectra show that the anhydride peak does not disappear, which supports the conclusion that perylene or naphthalic anhydride are not suitable curing agents at given conditions.

These results are also supported by literature in which various authors describe polyester formation with naphthalic anhydride and an epoxide that are only possible with sterically demanding metal complexes as catalysts.[52,53]

4.5 Amine fuctionalized perylenes as curing agents

In a second approach the synthesized amine functionalized perylene derivatives were used as curing agents for two epoxides. Therefore, **PDI-11** was reacted with monomer **EP1** as well as **BDDE**, whereas monomer **PDI-14** was reacted only with **EP1**.The molar ratio of amine-groups to epoxy groups was 1/2.

Polymers obtained from PDI-11 resulted in linear chains, since only one amine group was present and therefore crosslinking not possible, ehereas polymers formed with PDI-14 underwent crosslinking and insoluble networks were obtained. (Figure 26)

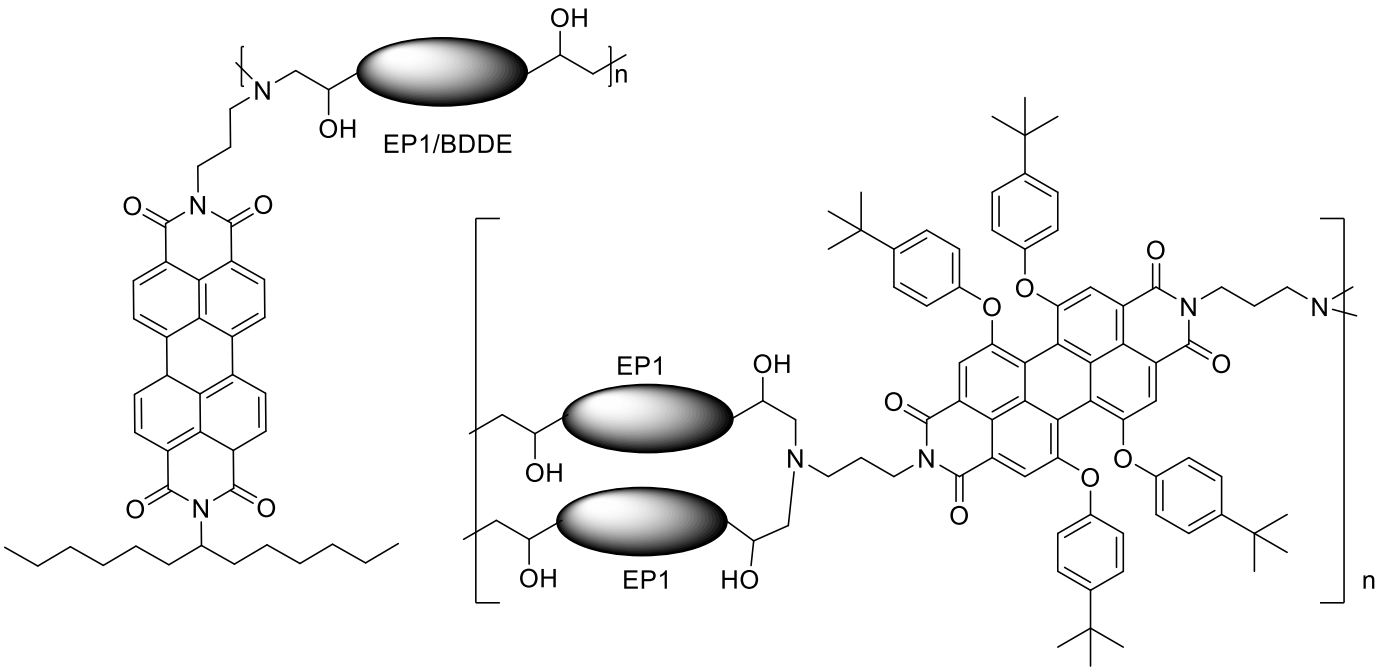

Figure 26: Chemical structures of epoxide EP1/BDDE cured with PDI-11 (left) and PDI-14 (right)

4.5.1 Polymer EP1PDI-11 and BDDEPDI-11

The synthesis was carried out according to the description in the experimental section. The obtained polymer stayed soluble in chlorobenzene and was measured by NMR and IR spectroscopy.

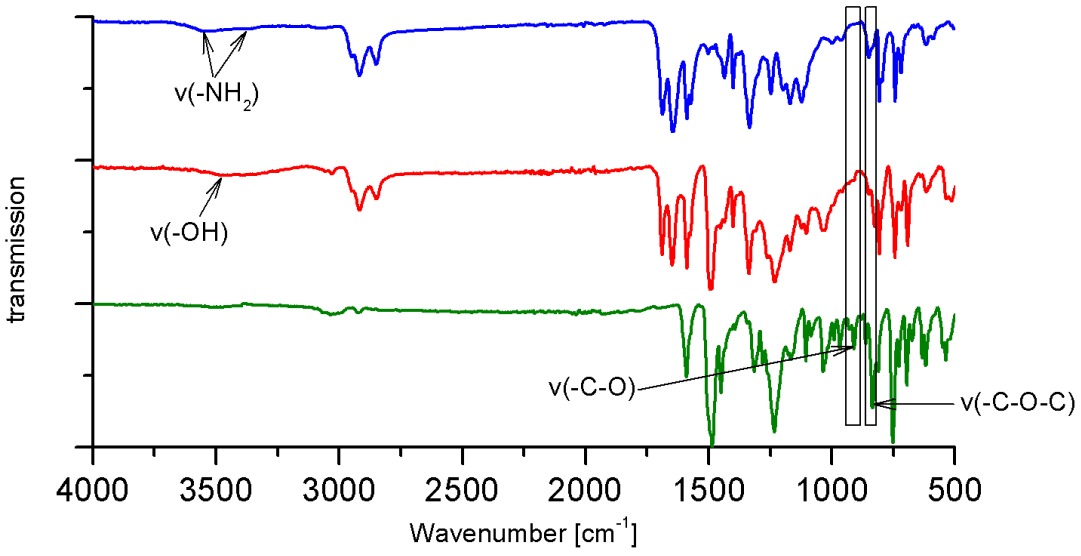

Figure 27: IR spectrum of monomer EP1 (green), diamine PDI-11 (blue) and polymer EP1PDI-11 (red)

Figure 27 shows the IR spectrum of the monomer **EP1**, amine **PDI-11**, and the polymer **EP1PDI-11**. The epoxy group peaks for **EP1** could be determined at 3033 cm^{-1}, 911 cm^{-1} and 836 cm^{-1}. The peak at 3033 cm^{-1} corresponds to the C-H stretch of the terminal oxirane group. The C-O deformation band of the oxirane group contributes to the peak at 911 cm^{-2} and the C-O-C stretch of the oxirane was determined at 836 cm^{-1}. All described peaks can be seen to disappear for the polymeric spectrum.
Furthermore, it can be seen that in the polymeric spectra the NH_2 peak at 3500 cm^{-1} and 3370 cm^{-1} is missing indicating a successful polymerization reaction. Also, a broad peak at around 3400 cm^{-1} has formed corresponding to the OH stretch peak, showing the formation of hydroxy groups. The NH bend vibrations for primary amines, could not be observed to disappear in IR, because of the overlay of the C-C aromatic stretch peak.[50,51,54]

Figure 28 shows the IR spectrum of monomer **BDDE**, amine **PDI-11** and polymer **BDDEPDI-11**. The same changes as discussed for polymer EP1PDI-11 apply, only slightly different wavenumbers for the characteristic epoxy peaks were observed for the epoxy monomer. For **BDDE** the epoxy peaks are at 3060-2998 cm^{-1}, 913 cm^{-1} and 840 cm^{-1} .[50,54,55] These peaks are missing in the spectrum of the polymer proving the successful reaction.

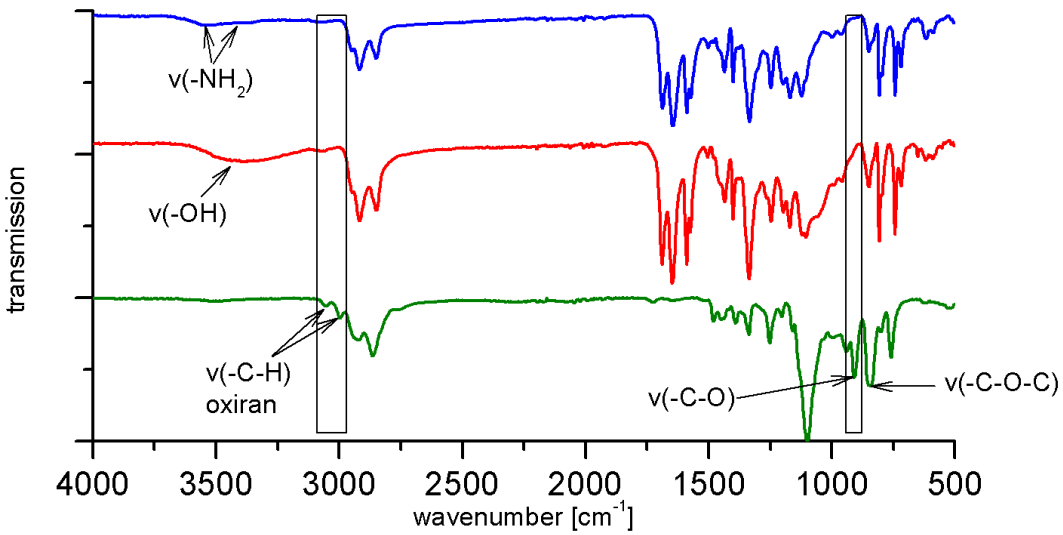

Figure 28: IR spectrum of monomer BDDE (black), diamine PDI-11 (blue) and polymer BDDEPDI-11 (red)

The obtained polymers were soluble and could therefore be characterized by means of ^{1}H-NMR spectroscopy (Figure 29). The reaction of the monomer with the amine, resulted in the following spectral changes.

It can be seen that the signals associated with the protons of the oxirane ring[54,56] (a,b,c) have disappeared, whereas new signals have evolved for the cured epoxy polymer in the range of 2.5-1.5 and 4.5-3.5 ppm . However, it was not possible to make a complete peak assignment for the polymeric compound because of the strong overlap of different peaks. The peaks of the monomers could be assigned by means of 2D COSY spectra. Furthermore, we can see that the peaks of the protons further away from the reactive region also show a shift, but a much smaller one. For both polymers the listed shifts are the same. The CH group next to the imide nitrogen (i) was shifted from 5.10 ppm to 5.18 ppm. The protons of the aromatic region of perylene were shifted from 8.42 ppm to 8.59 ppm and from 8.24 ppm to 8.42 ppm. The OH-peak was not visible.
All described observations indicate that the polymeric reaction worked properly and the polymeric compounds did form.

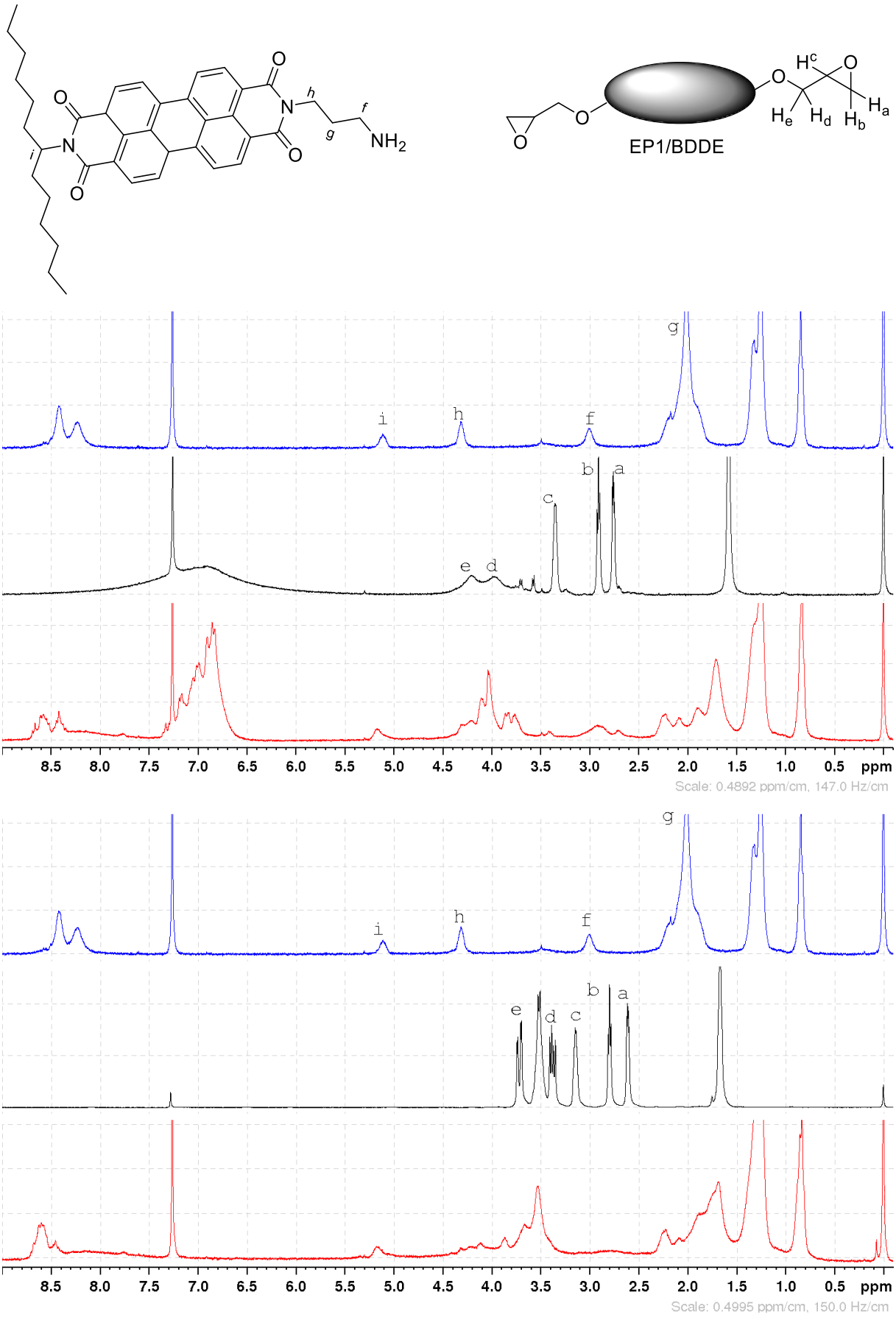

Figure 29:Top: ^{1}H NMR spectrum of polymer EP1PDI-11 (red), EP1 (black) and PDI-11 (blue)
Bottom: ^{1}H NMR spectrum of polymer BDDEPDI-11 (red), BDDE (black) and PDI-11 (blue)

4.5.2 Polymer EP1PDI-14

Monomer **PDI-14** was reacted only with **EP1**. The synthesis was carried out as described in the experimental section. The reaction mixture started to solidify after 5h. The obtained polymer was washed with dichloromethane until all soluble impurities were removed. The polymer underwent crosslinking and therefore it was not soluble anymore and characterization was only done by means of IR-spectroscopy.

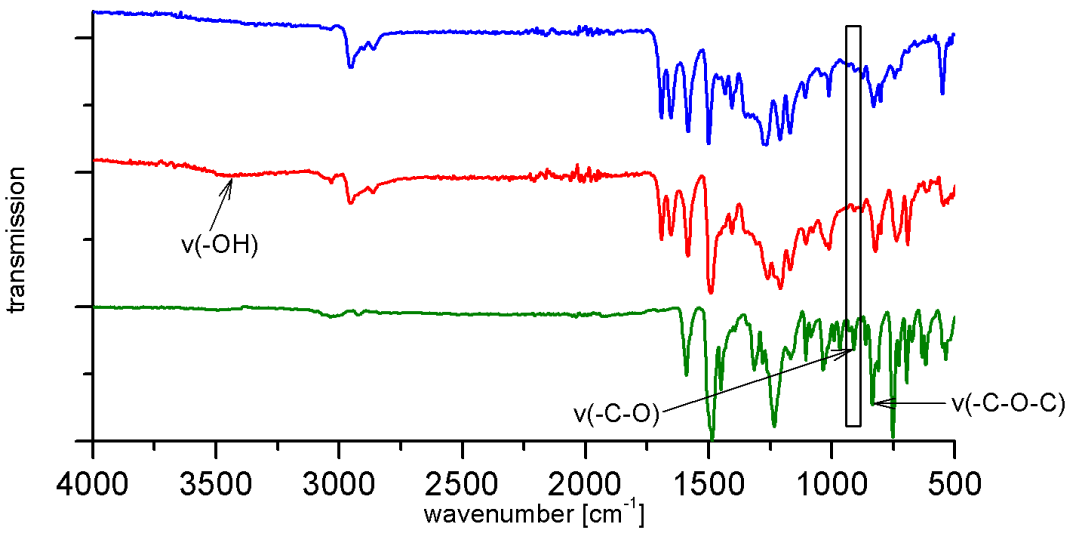

Figure 30: IR spectra of monomer EP1 (black), diamine PDI-11 (blue) and polymer EP1PDI-14 (red)

Since the primary amine peak is not visible in the IR spectrum of PDI-14, it was not possible to observe its disappearance. However, the polymeric spectrum shows the formation of the broad OH stretch peak at around 3400 cm^{-1}. The disappearance of the C-O deformation peak, at 913 cm^{-1}, of the oxirane group could also be observed. Therefore, it can be concluded, that the crosslinking worked properly, and an insoluble polymeric network has formed.

4.6 TGA measurements

All polymers were investigated by means of thermo gravimetric analysis. Figure 31 shows the TGA graphs of all synthesized polymers. The decomposition temperatures are given in Table 5.

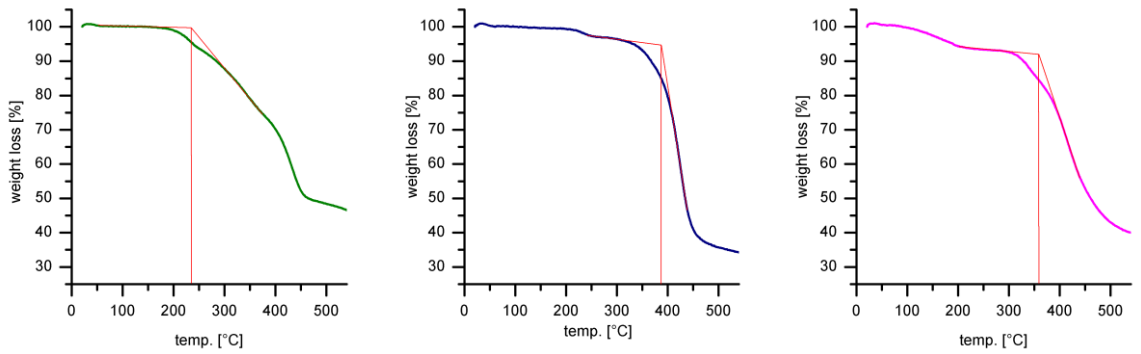

Figure 31: TGA graphs of BDDEPDI-11 (green), EP1PDI-11 (blue) and EP1PDI-14 (lila)

Table 5: Decomposition temperatures of polymer EP1PDI-11, BDDEPDI-11 and EP1PDI-14

compound	**Temperature of onset decomposition [°C]**
EP1PDI-11	390
BDDEPDI-11	230
EP1PDI-14	360

As it can be seen BDDEPDI-11 is stable up to 230°C. Changing the epoxide from BDDE to EP1, increases the stability from 230°C to 390°C for polymer EP1PDI-11. Polymer EP1PDI-14 also shows a high thermal stability with a decomposition temperature of 360°C.

The mass losses between 100 and 200°C for polymer EP1PDI-14 is attributed to the evaporation of solvent residues.

4.7 Solar cell characterization

The synthesized polymers were also investigated regarding to their photovoltaic response. Therefore, they were tested as active material in organic photovoltaics.

Polymer **EP1PDI-11** was used as single active material, because in theory it should be possible that EP1 acts as donor material and PDI-11 acts as acceptor material. It has to be mentioned, that in this particular case, the PDI acts as absorber and electron accepting material, whereas the triarylfunction of the EP1 should act as donor and easy oxidizeable compound.

Polymer **BDDEPDI-11** was used as polymer acceptor in an all-polymer solar cell. The polymeric donor for this cell was **PBDB-T**. Again, the polymer was not tailored to be the perfect acceptor polymer, it was a simple proof of concept. The major problem with all polymer solar cells, is that they tend to phase separate. Therefore to obtain an all polymer solar cell with high efficiencies the polymers have to be designed in a way that the phase separation can be controlled and no extreme phase separation takes place.[57]

4.7.1 J-V characterization

In the following part the J-V measurement of the built solar cells will be discussed.

EP1PDI-11:

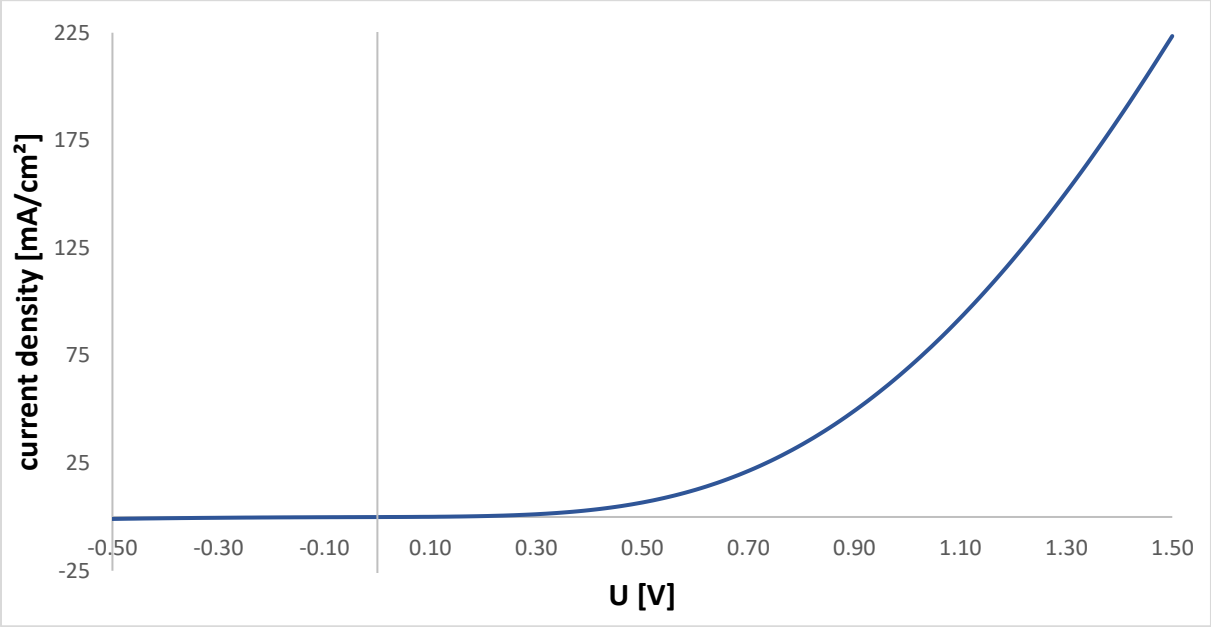

Figure 32: J-V measurement of EP1PDI-11 under illumination

Figure 32 shows one exemplary J-V curve for **EP1PDI-11**. It can be seen that the current density simply goes to zero with decreasing voltage and therefore no power conversion did take place.

Since the cell did not show a power conversion at all, it was not further investigated. It can be said that the donor-acceptor polymer EP1PDI-11 is not suitable as single active material in organic photovoltaics.

BDDEPDI-11 / PBDB-T

Figure 33 shows an exemplary J-V curve of a cell with **BDDEPDI-11 / PBDB-T** as active layer. The influence of different layer thicknesses and of annealing of the substrates was investigated. All results can be seen in Table 6.

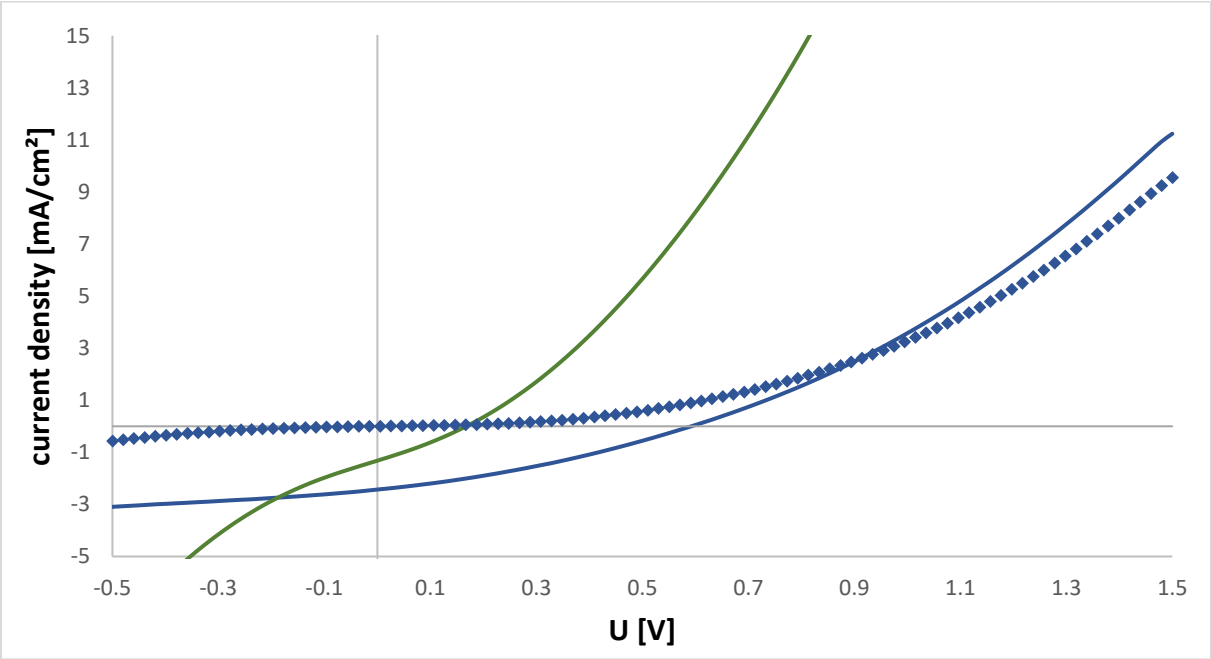

Figure 33: J-V curve of BDDEPDI-11 spincoated with 4000 rpm and 500 rpm/s: — not annealed illuminated, ♦ not annealed dark, — annealed illuminated.

Table 6: Comparison of the mean V_{OC}, J_{SC}, FF and PCE values at different spincoating rotation speeds with a standard acceleration of 500rpm/s

x [rpm]	annealing temp	thickness [nm]	V_{OC} [V]	J_{sc} [mA/cm²]	FF [%]	PCE [%]
1000	150 °C	113±8	0.12±0.01	0.83±0.1	26.7±0.1	0.026±0.005
1000	-	115 ±8	0.32±0.009	0.64±0.03	31.5±0.9	0.066±0.005
2000	150 °C	67±8	0.15±0.001	1.42±0.07	29.5±0.3	0.063±0.004
2000	-	78±4	0.49±0.07	2.22±0.1	34.6±2	0.37±0.03
3000	150 °C	82±2	0.14±0.009	1.53±0.1	27.6±1	0.060±0.006
3000	-	80±3	0.57±0.02	2.34±0.05	32.9±0.6	0.44±0.01
4000	150 °C	83±2	0.16±0.01	1.39±0.08	28.7±1	0.06±0.008
4000	-	86±2	0.56±0.03	2.09±0.33	32.7±2	0.38±0.07

The best cell achieved a PCE of 0.44±0.01%, with an FF of 32.9±0.6%.

The PCE increases with higher spincoating speed reaching its maximum at 3000rpm. On the one hand this could be due to the creation of a smoother surface and generally thinner layer at higher rpm. On the other hand this could result from the faster evaporation of chlorobenzene resulting in the fact that the polymers do not have time to undergo phase separation.[57]

The samples were also annealed at 150°C for 15 min. In many cases annealing has a positive influence on the efficiency of the solar cells[58].

However, as seen in Figure 33, the annealed cells, do not show a typical J-V curve. The curve looks more like one of a conductor than of a semiconductor, indicating that the cell is short-circuited. Since only the annealed cells showed a short-circuit it is believed, that annealing at these conditions, lead to a phase separation of the polymers, leading to “cracks” in the active layer. Those cracks then are responsible, that the cathode gets in contact with the anode and a short circuit is produced.
Another possibility would be that the synthesized polymer **BDDEPDI-11** is so conductive that, after phase separation, the polymer itself short-circuited the cell.

To make sure that the measured PCE´s did not originate only from either the donor or the acceptor material, cells were built with either only the donor or only the acceptor as active material and measured, showing that neither one exhibited PCEs worth mentioning.
The cell built only with **BDDEPDI-11** as active material, showed a short circuit from the beginning even without annealing. This fact supports the before mentioned theory, of the conductivity of the polymer.
However, there is also the possibility, that the polymer did aggregate, and therefore free channels in the active layer were provided and the cathode got into contact with the anode leading to a short circuit.
To proof what is really going on, further investigation would be needed, for which there was no time during this work.

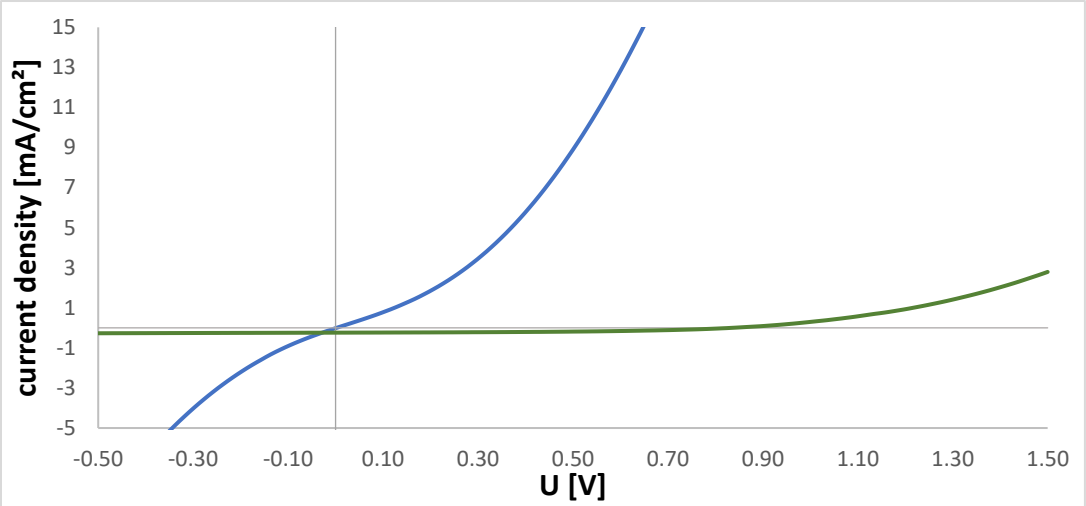

Figure 34: J-V curve of only BDDEPDI-11 (blue) and only PBDB-T (green) both under illumination

5. Summary and outlook

The aim of this work was the synthesis of perylene functionalized epoxy resins. Two approaches were performed. **i)** the use of perylene carboxylic anhydride derivatives **ii)** the use of amine functionalized perylene derivatives as curing agents. Therefore, the focus was on the synthesis of the perylene monomers and their use to cure epoxy monomers. Furthermore, the photoresponse of the final polymers was investigated in solar cells.

In a first step the bay positions of PTCDA were nitrated, to obtain the 1,6- and 1,7-dinitroperylene-3,4,9,10 tetracarboxylic dianhydride isomeric mixture. The nitro-groups should on the one hand increase the solubility and on the other hand improve the optical performance. Soon it has been seen that the nitro-group is very reactive and therefore unexplained side reactions occurred when trying to polymerize the nitrated PTCDA. Therefore, those derivatives were not further investigated.

The polymerization then was carried out with tetra-bromo substituted PTCDA, since the bromo substituents should weaken the π-π stacking and therefore make the compound more soluble.
It has been seen that the use of perylene carboxylic anhydrides as curing agents proved not to be possible in this work.
Initially, it was thought that polymerization could not occur because the solubility of the tetra-bromo substituted PTCDA was still too weak. Therefore, a more soluble perylene anhydride derivative was synthesized by imidization of PTCDA and selective hydrolysis to obtain a perylene monoimide-monoanhydride derivative (**PMI-9**). It has been seen, that also with the more soluble PMI-9, curing of epoxy monomers was not possible. After several model reactions, it could be concluded, that the anhydride group of the perylene is not reactive enough and only homopolymerization of the epoxy monomer occurred. IR-spectroscopy of the polymerization products showed the disappearance of the anhydride group. This disappearance could be explained with hydrolysis taking place rather than reaction with the epoxide.
Since all polymerization attempts with anhydride did fail, it was decided to pursue only the second approach.

Two amine functionalized perylenes were synthesized (PDI-11 and PDI-14). PDI-11 has no bay substituents. To increase its solubility, the compound has only one reactive amine group, and the second imide comprises of long bulky alkyl chains.
The synthesis of PDI-11 worked without complications in a straight-forward way.
The bay region of PDI-14 is substituted with bulky phenyl groups to increase its solubility. So, it was possible two get one amine functionality at each imine resulting in a total of two. The main challenge for the synthesis of PDI-14 turned out to be the purification because the side products have very close together spots on TLC. Purification of PDI-14 was not possible.
The synthesized PDI´s were investigated by means of NMR and IR spectroscopy.

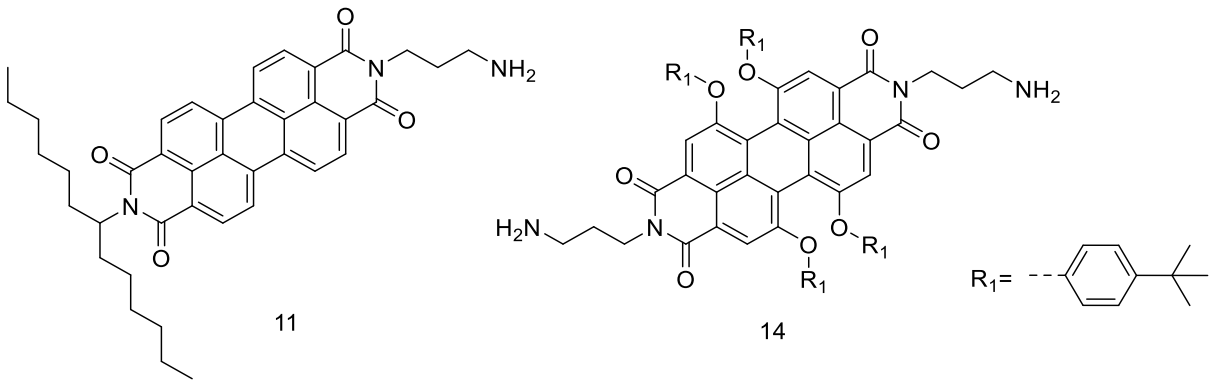

Figure 35: structure of PDI-11 and PDI-14

PDI-11 was used to cure BDDE and EP1 monomers. Since PDI-11 only has one amine functionality, soluble linear polymers were obtained, which were investigated by means of NMR and IR spectroscopy.
PDI-14 was used to only cure the EP1 monomer. The diamine functionalized PDI-14 built insoluble crosslinked polymers and was only investigated by IR spectroscopy.

To investigate the photovoltaic performance, polymers BDDEPDI-11 and EP1PDI-11 were incorporated as active material in organic solar cells.
EP1PDI-11 should work as a donor-acceptor polymer were the TPPD moieties of EP1 work as donor and the perylene moieties of PDI-11 work as acceptor. The cells did not show any power conversion efficiencies at all. Therefore, it can be said, that the proof of concept did fail, and the polymer is not suitable to be used in single active material OPV´s.

BDDEPDI-11 showed PCE´s of maximal 0.44%, which is very low for all polymer solar cells, since they have already exceeded PCE´s of 10%[59]. Furthermore, after annealing, the cells showed short circuit behavior.
Those weak performances make the two polymers not very promising for further solar cell applications.

However, these perylene functionalized epoxy resins should further be investigated **a)** with regard to their thermal conductivity and – in the case of additional triarylamine-cofunctionalization **b)** with regard to their electrochemical performance in using them as electrode material in polymer batteries.

6. References

1. Ren, L.; Wang, M.; Wei, Z.; Cheng, J.; Liu, K.; Pan, L.; Lao, L.; Lu, S.; Yu, J. *New J. Chem.* **2020**, *44*, 9337–9343.
2. Borba Marchetto, D.; Carneiro Moreira, D.; Ribatski, G. A REVIEW ON POLYMER HEAT SINKS FOR ELECTRONIC COOLING APPLICATIONS. In 17th Brazilian Congress of Thermal Sciences and Engineering; ABCM, November 2018.
3. Hussain, A.R.J.; Alahyari, A.A.; Eastman, S.A.; Thibaud-Erkey, C.; Johnston, S.; Sobkowicz, M.J. *Applied Thermal Engineering* **2017**, *113*, 1118–1127.
4. Liang, S.; Gui, D.; Zhang, W.; Xiong, W.; Liu, J. Improving the thermal and mechanical properties of epoxy resins for electronic packaging. In 2014 15th International Conference on Electronic Packaging Technology; IEEE, August 2014 - August 2014, pp 191–195.
5. Henry, A. *Annual Rev Heat Transfer* **2014**, *17*, 485–520.
6. Shen, S.; Henry, A.; Tong, J.; Zheng, R.; Chen, G. *Nature nanotechnology* **2010**, *5*, 251–255.
7. Hansen, D.; Bernier, G.A. *Polym. Eng. Sci.* **1972**, *12*, 204–208.
8. Xu, Y.; Wang, X.; Zhou, J.; Song, B.; Jiang, Z.; Lee, E.M.Y.; Huberman, S.; Gleason, K.K.; Chen, G. *Science advances* **2018**, *4*, eaar3031.
9. Akatsuka, M.; Takezawa, Y. *J. Appl. Polym. Sci.* **2003**, *89*, 2464–2467.
10. Würthner, F.; Saha-Möller, C.R.; Fimmel, B.; Ogi, S.; Leowanawat, P.; Schmidt, D. *Chemical reviews* **2016**, *116*, 962–1052.
11. Epoxy Resins Market Share, Size, Trends, Industry Analysis Report By Formulation Type (DGBEA, DGBEF, Novolac, Aliphatic, Glycidylamine, and, Others); By Application (Paints & Coatings, Adhesives, Composites, Electrical & Electronics, Wind Turbines, and Others); By Regions, Segments & Forecast, 2020 - 2026. Available online: https://www.polarismarketresearch.com/industry-analysis/epoxy-resins-market (accessed on 30 August 2020).
12. Epoxy Resin Market Size, Share, and Trends Analysis Report, By Application (Paints & Coatings, Wind Turbine, Composites, Construction, Electrical &

Electronics, Adhesives) And Segment Forecasts To 2024. Available online: https://www.grandviewresearch.com/industry-analysis/epoxy-resins-market#:~:text=Industry%20Insights,the%20global%20epoxy%20resins%20demand. (accessed on 30 August 2020).

13. Ellis B. Chemistry and Technology of Epoxy Resins; Springer Netherlands: Dordrecht, **1992**.
14. Pham, H.Q.; Marks, M.J. In Ullmann's Encyclopedia of Industrial Chemistry 2000; Epoxy Resins.
15. Varma, I.K.; Gupta, V.B. In Comprehensive Composite Materials 2000; Thermosetting Resin—Properties, pp 1–56.
16. Shechter, L.; Wynstra, J. *Ind. Eng. Chem.* **1956**, *48*, 86–93.
17. Licari, J.J.; Swanson, D.W. Adhesives technology for electronic applications: Materials, processing, reliability; William Andrew Pub: Waltham MA, **2011**.
18. K. Frantisek, S.J. *Acta. Geodyn. Geomater* **2007**, *4*, 85–92.
19. Fisch, W.; Hofmann, W.; Koskikallio, J. *J. Appl. Chem.* **1956**, *6*, 429–441.
20. Dearborn, E.C.; Fuoss, R.M.; White, A.F. *J. Polym. Sci.* **1955**, *16*, 201–208.
21. Fischer, R.F. *J. Polym. Sci.* **1960**, *44*, 155–172.
22. Matějka, L.; Lövy, J.; Pokorný, S.; Bouchal, K.; Dušek, K. *J. Polym. Sci. Polym. Chem. Ed.* **1983**, *21*, 2873–2885.
23. Trappe, V.; Burchard, W.; Steinmann, B. *Makromolekulare Chemie. Macromolecular Symposia* **1991**, *45*, 63–74.
24. Steinmann, B. *J. Appl. Polym. Sci.* **1989**, *37*, 1753–1776.
25. Tanaka, Y.; Kakiuchi, H. *J. Appl. Polym. Sci.* **1963**, *7*, 1063–1081.
26. Tanaka, Y.; Kakiuchi, H. *J. Polym. Sci. A Gen. Pap.* **1964**, *2*, 3405–3430.
27. Herbst, W.; Hunger, K. Industrial Organic Pigments: Production, Properties, Applications; Wiley-VCH: Weinheim, **2006**.
28. Huang, C.; Barlow, S.; Marder, S.R. *The Journal of organic chemistry* **2011**, *76*, 2386–2407.

29. Lee, S.K.; Zu, Y.; Herrmann, A.; Geerts, Y.; Müllen, K.; Bard, A.J. *J. Am. Chem. Soc.* **1999**, *121*, 3513–3520.

30. Leroy-Lhez, S.; Perrin, L.; Baffreau, J.; Hudhomme, P. *Comptes Rendus Chimie* **2006**, *9*, 240–246.

31. Xiong, W.; Meng, X.; Liu, T.; Cai, Y.; Xue, X.; Li, Z.; Sun, X.; Huo, L.; Ma, W.; Sun, Y. *Organic Electronics* **2017**, *50*, 376–383.

32. Yin, Y.; Yang, J.; Guo, F.; Zhou, E.; Zhao, L.; Zhang, Y. *ACS applied materials & interfaces* **2018**, *10*, 15962–15970.

33. Kolcu, F.; Çulhaoğlu, S.; Kaya, İ. *Progress in Organic Coatings* **2019**, *137*, 105284.

34. Pan, L.; Lu, S.; Xiao, X.; He, Z.; Zeng, C.; Gao, J.; Yu, J. *RSC Adv.* **2015**, *5*, 3177–3186.

35. Bonger, K.M.; Hoogendoorn, S.; van Koppen, C.J.; Timmers, C.M.; Overkleeft, H.S.; van der Marel, G.A. *ChemMedChem* **2009**, *4*, 2098–2102.

36. Hu, Y.; Chen, S.; Zhang, L.; Zhang, Y.; Yuan, Z.; Zhao, X.; Chen, Y. *The Journal of organic chemistry* **2017**, *82*, 5926–5931.

37. Schwartz, E.; Palermo, V.; Finlayson, C.E.; Huang, Y.-S.; Otten, M.B.J.; Liscio, A.; Trapani, S.; González-Valls, I.; Brocorens, P.; Cornelissen, J.J.L.M.; Peneva, K.; Müllen, K.; Spano, F.C.; Yartsev, A.; Westenhoff, S.; Friend, R.H.; Beljonne, D.; Nolte, R.J.M.; Samorì, P.; Rowan, A.E. *Chemistry (Weinheim an der Bergstrasse, Germany)* **2009**, *15*, 2536–2547.

38. Würthner, F.; Hanke, B.; Lysetska, M.; Lambright, G.; Harms, G.S. *Organic letters* **2005**, *7*, 967–970.

39. Yu, X.; Zhan, C.; Zhang, S.; Tang, A.; Zhang, X.; Huang, Y.; Yao, J. *Asian Journal of Organic Chemistry* **2013**, *2*, 54–59.

40. Choy, W.C.H. Organic solar cells: Materials and device physics; Springer: London, Heidelberg, **2013**.

41. Hao, L.; Jiang, W.; Wang, Z. *Tetrahedron* **2012**, *68*, 9234–9239.

42. Tsai, H.-Y.; Chang, C.-W.; Chen, K.-Y. *Molecules (Basel, Switzerland)* **2013**, *19*, 327–341.

43. Berns, B.; Tieke, B. *Polym. Chem.* **2015**, *6*, 4887–4901.

44. Fukumoto, H.; Nakajima, H.; Kojima, T.; Yamamoto, T. *Materials (Basel, Switzerland)* **2014**, *7*, 2030–2043.

45. Glenn Facey. Chemical Exchange Agents to simplify NMR Spectra (accessed on 15 December 2020).

46. Saeedi, I.A.; Andritsch, T.; Vaughan, A.S. *Polymers* **2019**, *11*.

47. Socrates, G. Infrared and Raman characteristic group frequencies: Tables and charts; John Wiley & Sons LTD: Chichester [etc.], **2015**.

48. Chen, K.-Y.; Chow, T.J. *Tetrahedron Letters* **2010**, *51*, 5959–5963.

49. Rocard, L.; Goujon, A.; Hudhomme, P. *Molecules (Basel, Switzerland)* **2020**, *25*.

50. Celina, M.C.; Giron, N.H.; Rojo, M.R. *Polymer* **2012**, *53*, 4461–4471.

51. IR spectroscopy tutorial. Available online: http://www.orgchemboulder.com/Spectroscopy/irtutor/tutorial.shtml (accessed on 29 November 2020).

52. Ryu, H.K.; Bae, D.Y.; Lim, H.; Lee, E.; Son, K.-s. *Polym. Chem.* **2020**, *11*, 3756–3761.

53. Peña Carrodeguas, L.; Martín, C.; Kleij, A.W. *Macromolecules* **2017**, *50*, 5337–5345.

54. David Beichel. Tuneable Redox-Active Polymer Network for Organic Batteries. Dissertation: Graz, Technische Universität Graz, **2019**.

55. Bao, L.; Fan, H.; Chen, Y.; Yan, J.; Zhang, J.; Guo, Y. *Adv Polym Technol* **2018**, *37*, 906–912.

56. Camara, F.; Benyahya, S.; Besse, V.; Boutevin, G.; Auvergne, R.; Boutevin, B.; Caillol, S. *European Polymer Journal* **2014**, *55*, 17–26.

57. Benten, H.; Mori, D.; Ohkita, H.; Ito, S. *J. Mater. Chem. A* **2016**, *4*, 5340–5365.

58. Biber, M.; Aydoğan, Ş.; Çaldıran, Z.; Çakmak, B.; Karacalı, T.; Türüt, A. *Results in Physics* **2017**, *7*, 3444–3448.

59. Fan, Q.; An, Q.; Lin, Y.; Xia, Y.; Li, Q.; Zhang, M.; Su, W.; Peng, W.; Zhang, C.; Liu, F.; Hou, L.; Zhu, W.; Yu, D.; Xiao, M.; Moons, E.; Zhang, F.; Anthopoulos, T.D.; Inganäs, O.; Wang, E. *Energy Environ. Sci.* **2020**, *13*, 5017–5027.

7. Appendix

7.1 Abbreviations

ATR-IR	attenuated total reflectance-infrared spectroscopy
BDDE	1,4-butanedioldiglycidylether
CH	cyclohexane
DCM	dichloromethane
DMA	dimethylaniline
DMAc	N,N-dimethylacetamide
ETL	electron transport layer
Et_3N	triethylamine
EtOAc	ethyl acetate
FF	fill factor
HTL	hole transport layer
ITO	indium tin oxide
J_{sc}	short circuit current density
MHHPA	Hexahydromethylphthalsäureanhydrid
OPV	organic photovoltaic
PBDB-T	Poly[[4,8-bis[5-(2-ethylhexyl)-2-thienyl]benzo[1,2-b:4,5-b´]dithiophene-2,6-diyl]-2,5-thiophenediyl[5,7-bis(2-ethylhexyl)-4,8-dioxo-4H,8H-benzo[1,2-c:4,5-c´]dithiophene-1,3-diyl]] polymer
PCE	power conversion efficiency
PDA/PTCDA	3,4,9,10-Perylen-tetracarbonsäure-dianhydrid
RT	room temperature
TFA	trifluoro acetic acid
TGA	thermo gravimetric analysis
THF	tetrahydrofuran
TLC	thin layer chromatography
TPPD	N^1,N^1,N^4,N^4-tetraphenyl-p-phenylenediamine

7.2 List of figures

7.3 List of schemes

7.4 List of tables